

# Absence of ubiquitinated inclusions in hypocretin neurons of patients with narcolepsy

M. Honda, MD, PhD  
T. Arai, MD, PhD  
M. Fukazawa  
Y. Honda, MD, PhD  
K. Tsuchiya, MD, PhD  
A. Salehi, MD, PhD  
H. Akiyama, MD, PhD  
E. Mignot, MD, PhD

Address correspondence and reprint requests to Dr. Makoto Honda, Sleep Disorders Research Project, Tokyo Institute of Psychiatry, 2-1-8 Kamikiazawa, Setagaya-ku, Tokyo 156-8585, Japan  
honda@pii.tycho.jp

## ABSTRACT

**Objectives:** The cause of hypocretin cell loss in human narcolepsy–cataplexy is unknown but has been suggested to be neurodegenerative in nature. To test this hypothesis, we evaluated the remaining hypocretin cells in human narcolepsy brains for the presence of aggregated protein inclusions, gliosis, and inflammation.

**Methods:** Brains were examined by routine histologic methods for potential comorbid neurodegenerative diseases and through immunohistochemical screening for protein inclusions in the hypothalamus. Hypothalamic sections of 4 subjects with narcolepsy and 5 nonneurologic controls were examined immunohistochemically with antibodies against ubiquitin (a marker of aggregated protein), allograft inflammatory factor 1 (AIF1, a microglial activation marker), glial fibrillary acidic protein (GFAP, a reactive astrocytic marker), and hypocretin. Hypothalami of subjects with narcolepsy were additionally examined for the presence of known components of protein aggregates (tau,  $\alpha$ -synuclein, amyloid  $\beta$ , and TDP-43).

**Results:** Hypocretin cells were markedly decreased in all 4 subjects with narcolepsy. Ubiquitinated inclusions were not observed in the total of 96 remaining hypocretin cells in these subjects. Further, we noted that even in patients with dementia neuropathology, the lateral hypothalamic hypocretin area was spared from ubiquitinated inclusions. AIF1 and GFAP staining in the perifornical area was unremarkable.

**Conclusions:** Our findings suggest that hypocretin cell loss does not involve ubiquitinated inclusions, the hallmark of most neurodegenerative diseases. The lack of increased markers of inflammation also argues against a progressive and continuous neurodegenerative process. *Neurology* 2009;73:511–517

## GLOSSARY

(AD) = neuropathologically consistent with Alzheimer disease, AIF1 = allograft inflammatory factor 1, CERAD = Consortium to Establish a Registry for Alzheimer's Disease, DAB = diaminobenzidine, Fx = fornix, GFAP = glial fibrillary acidic protein, IgG = immunoglobulin G, LBD = Lewy body disease, NA = not available, NFT = neurofibrillary tangle, PBS = phosphate-buffered saline, PLM = periodic leg movement, PMI = postmortem interval, PSG = polysomnography, REML = REM latency, SL = sleep latency, SOREMP = sleep onset REM period, 3V = third ventricle.

Studies in animals and humans have shown that narcolepsy–cataplexy is caused by impaired hypocretin (also called orexin) neurotransmission.<sup>1,2</sup> Impaired hypocretin transmission due to single hypocretin gene mutations is rare in humans.<sup>1</sup> Rather, in most cases of narcolepsy with cataplexy, hypothalamic hypocretin cells are lost through an unknown and highly selective process that does not alter the closely intermingled melanin-concentrating hormone cell population.<sup>1,2</sup> Speculation on the causes of this cell loss have included an autoimmune process (based on the tight HLA-DQB1\*0602 association) or degeneration of hypocretin neurons.<sup>3</sup> Repeated attempts to identify an autoimmune process have so far failed,<sup>4</sup> suggesting that it is necessary to explore other potential mechanisms.

In neurodegenerative disorders, specific neuronal subtypes are often affected by a process associated with the accumulation of intracellular protein aggregates, but whether these aggre-

From the Sleep Disorder Research Project (M.H., M.F.) and Psychogeriatric Research Project (T.A., H.A.), Tokyo Institute of Psychiatry, Setagaya-ku, Tokyo, Japan; Japan Somnology Center (M.H., Y.H.), Neuropsychiatric Research Institute, Tokyo, Japan; and Tokyo Metropolitan Matsuzawa Hospital (K.T.), Department of Neurology (A.S.) and Narcolepsy Center (E.M.), Stanford University, Palo Alto, CA.

*Disclosure:* Author disclosures are provided at the end of the article.

**Table Demographic data regarding brains used in this study**

	Diagnosis	Age, y	Sex	Ethnicity	Cause of death	Neuropathologic diagnosis	PMI, h
N1	Narcolepsy	69	M	Japanese	Epidural hematoma	—	10.0
N2	Narcolepsy	75	M	Japanese	Spinal cord infarction, prostate cancer metastasis, sepsis	(AD)	5.5
N3	Narcolepsy	89	F	White	NA	LBD	20.0
N4	Narcolepsy	79	F	Japanese	Chronic renal failure, heart failure, melena	Senile dementia of the NFT type	3.0
C1	Control	84	F	Japanese	Heart failure, kidney carcinoma	—	8.8
C2	Control	70	F	Japanese	Status asthmaticus	—	7.5
C3	Control	79	M	White	Aging (heart failure)	—	6.5
C4	Control	84	F	White	NA	—	NA
C5	Control	67	M	Japanese	Lung cancer, malnutrition, hydrothorax	—	4.0

PMI = postmortem interval; (AD) = neuropathologically consistent with Alzheimer disease (Consortium to Establish a Registry for Alzheimer's Disease diagnosis NP possible b); LBD = Lewy body disease; NFT = neurofibrillary tangle; NA = not available.

gates cause cell death or protect against neurodegeneration remains unresolved. These aggregates generally contain ubiquitin, a "tag" that is added to proteins that are targeted for degradation.<sup>5</sup> Recently, analysis of ubiquitinated protein revealed the novel TDP-43 protein as a cause of amyotrophic lateral sclerosis.<sup>6,7</sup> Hypocretin cell numbers are decreased in several neurodegenerative disorders, including Parkinson disease,<sup>8,9</sup> multiple system atrophy,<sup>10</sup> and Huntington disease.<sup>11</sup> In these diseases, protein inclusions were identified in small numbers of hypocretin cells,<sup>8</sup> indicating that these cells can be affected by neurodegenerative processes. Ubiquitin-containing deposits have also been identified in the hypothalamus of patients with Niemann–Pick disease type C,<sup>12</sup> a disorder known to cause secondary narcolepsy.

We hypothesized that hypocretin cell neurodegeneration occurs in narcolepsy, a process likely marked by the presence of protein aggregates. We examined rare remaining hypocretin cells of patients with narcolepsy for the presence of ubiquitinated inclusions, and potential astrocytic or microglial reactions, processes associated with active neurodegeneration. We also examined hypothalamic sections from 4 subjects with narcolepsy for the presence of known components of protein aggregates (tau,  $\alpha$ -synuclein, amyloid  $\beta$ , and TDP-43).

**METHODS** This study was approved by the ethical committees of the collaborative institutes. Written informed consent was

obtained from all patients or families. We examined brain tissue from 4 patients with narcolepsy (50% men, aged  $78 \pm 8$  years, 75% Japanese, postmortem interval [PMI]  $9.6 \pm 7.5$  hours) and 5 nonneurologic controls (2 men and 3 women, without a clinical history of unexplained excessive daytime sleepiness, aged  $77 \pm 8$  years, 60% Japanese, PMI  $6.7 \pm 2.0$  hours). None of these subjects were used in previous neuropathologic studies.<sup>12,13</sup> Demographic data are shown in the table. In most cases (7 of 9), brains were first studied by routine neuropathologic examination. Right brain hemispheres were fixed postmortem with 10% formalin, embedded in paraffin, and 8- $\mu$ m sections from cortices, hippocampus, basal ganglia, midbrain, and pons cerebellum were prepared. These sections were stained using the hematoxylin and eosin, Klüver–Barrera, methenamine silver, and Gallyas–Braak methods. We used Consortium to Establish a Registry for Alzheimer's Disease (CERAD) scoring<sup>14</sup> and Braak staging<sup>15</sup> when Alzheimer neuropathology was noted.

Seven brain blocks containing hypothalamus (3 narcolepsy and 4 controls) were also obtained and fixed in 4% paraformaldehyde, cut into 40- $\mu$ m cryosections and used for immunohistochemical staining. Hypothalamic structure orientation was determined using human atlas coordinates.<sup>16</sup> Four stained sections (spaced at approximately 800  $\mu$ m) covering the hypocretin cell-containing perifornical area, were selected. This area spans from the mammillary bodies (optic chiasm + 10 mm) to an area immediately proximal to where the fornix makes contact with the third ventricle (optic chiasm + 7 mm). Paraffin-embedded hypothalamic sections were used for immunostaining in the 2 subjects (1 narcolepsy and 1 control) whose hypothalamic tissue was unavailable in frozen sections. For these, representative 8- $\mu$ m thin coronal sections (corresponding to atlas figure 28, optic chiasm + 8 mm) were selected for evaluation.

Cryosectioned brain samples were permeabilized with 0.3% Triton X-100 in phosphate-buffered saline (PBS) for 4 weeks. All subsequent steps were performed on free-floating sections at 4°C, interspersed with washes in PBS buffer (5 minutes 3 times). Sections were 1) treated with 0.6% H<sub>2</sub>O<sub>2</sub> in PBS for 30 minutes; 2) blocked in 1.5% normal goat or horse serum in PBST (PBS + 0.25% Triton X-100) for 30 minutes; and 3) incubated in PBST for 24 hours with rabbit anti-ubiquitin polyclonal antibody (1:10,000, Z0458, Dako, Carpinteria, CA), rabbit anti-allograft inflammatory factor 1 (AIF1, also called ionized

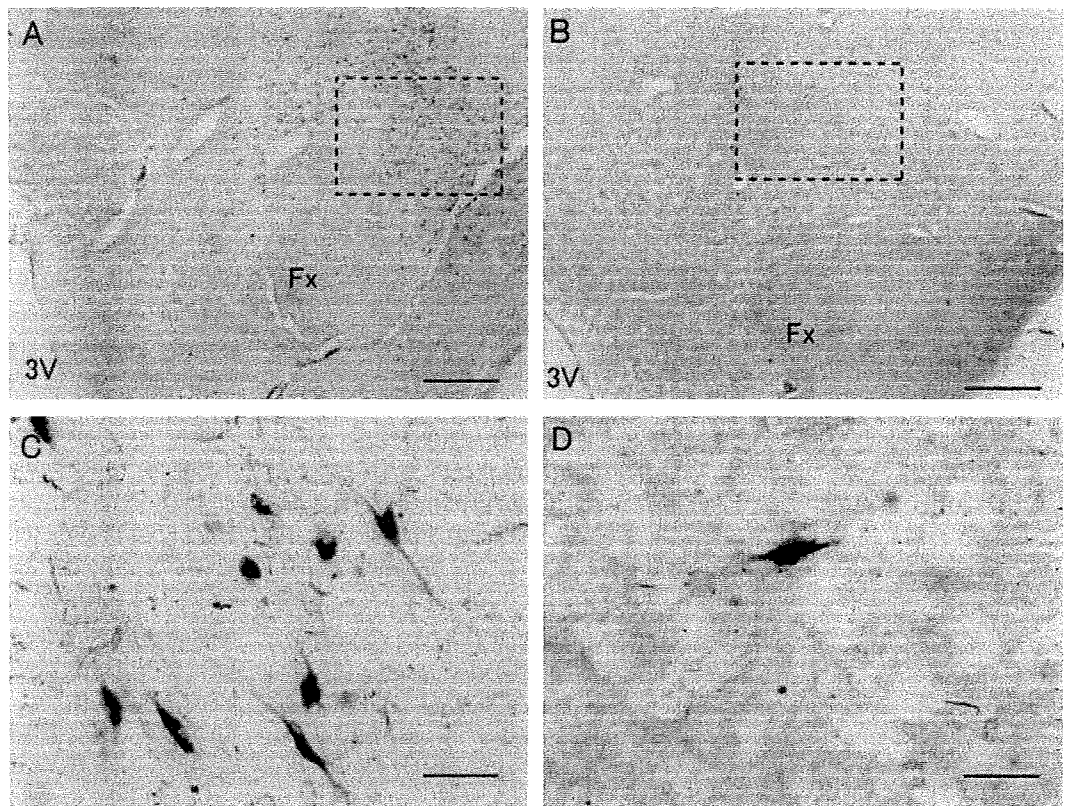
calcium binding adaptor molecule 1:1ba1) polyclonal antibody (1:5,000, 019-19741; Wako, Osaka, Japan), or rabbit anti-gliofibrillary acidic protein (GFAP) antibody (1:5,000, RB-087-A, Thermo, Fremont, CA) and a mouse anti-hypocretin monoclonal antibody (1:10,000 house made). Four narcolepsy hypothalamic sections were also stained with rabbit anti-phosphated tau polyclonal antibody (1:50,000, AP422<sup>17</sup>), rabbit anti- $\alpha$ -synuclein polyclonal antibody (1:5,000, 1175<sup>18</sup>), rabbit anti-amyloid  $\beta$  polyclonal antibody (1:20,000, E50<sup>19</sup>), mouse anti-phosphated TDP-43 monoclonal antibody (1:5,000, pS409/410<sup>20</sup>), anti-ubiquitin antibody (polyclonal antibody Z0458 or mouse monoclonal anti-ubiquitin antibody (1:5,000, MAB1510 clone FK1, Millipore, Bellerica, MA), and anti-phosphated tau polyclonal antibody (AP422) as well as anti-hypocretin monoclonal antibody; 4) incubated with biotinylated goat anti-rabbit immunoglobulin G (IgG) or horse anti-mouse IgG antibody (1:200, Vector Laboratories, Burlingame, CA) in PBST for 1 hour; 5) incubated in ABC reagents (Vector Laboratories) in PBST for 1 hour; and 6) preincubated in 0.25 mg/mL diaminobenzidine (DAB) or DAB with 1% nickel chloride in PBST for 15 minutes followed by the addition of H<sub>2</sub>O<sub>2</sub> as a final concentration of 0.02% for 15 minutes. Sections were then mounted and analyzed by microscopy, and an Olympus BX51 microscope (Olympus, Tokyo, Japan) equipped with charge-coupled device camera (DP70, Olympus) was used to take digital photographs of stained sections. Paraffin sections were first deparaffinized in xylene, hydrated, and stained on the slide according to the procedures described above.

**RESULTS Case reports.** Case N1 (a Japanese man) began working in a fish market at age 14 years, and recurrent daytime sleep episodes began at age 15 years. He slept frequently during work, unaware that he was affected by hypersomnia. His first cataplexy episode, at age 53 years, caused him to fall to the ground. Cataplexy occurred when he became excited or angry, and he resigned from work at age 60 years after dropping a special knife while cleaning a large fish with a fellow worker. His cataplexy continued to become aggravated, leading him to seek medical help, and he was diagnosed with narcolepsy at age 63 years. He rarely experienced hypnagogic hallucinations and sleep paralysis. His 1 nap polysomnography (PSG) at his initial visit showed shortened sleep latency (SL) and REM latency (REML) (2 minutes and 6 minutes), and indicated a sleep onset REM period (SOREMP). At age 66 years, he sustained a brain injury in a traffic accident, and MRI revealed a right frontal lesion. Subsequently, his unsteady walking led to frequent falls and injuries. He sometimes showed nocturnal occupational delirium and was hospitalized 3 times for the treatment of prolonged disoriented hallucinatory states. Nocturnal PSG at age 68 years showed lack of deep sleep but no signs of sleep apnea or periodic leg movements (PLMs). Cognitive function was not assessed, but memory disturbances were not noted when he was fully awake. He died of epidural hematoma, due to repeated head injury at age 69 years. Neuropathologic examination

revealed small numbers of neurofibrillary tangles (NFTs) in the hippocampus (Braak stage I) and senile plaques in the temporal cortex (Braak stage A, CERAD age-related plaque score B). Sparse ubiquitin-positive threads were observed in the ventral part of the posterior hypothalamus (premamillary area) but not in the lateral hypothalamic hypocretin area. No ubiquitin-positive inclusions were found in the 16 remaining hypocretin cells. Additional screening of hypothalamic sections for known protein aggregates revealed 1 NFT and several neuropil threads in premamillary area. There were no amyloid  $\beta$ -positive senile plaques,  $\alpha$ -synuclein-positive inclusions, Lewy neurites, TDP-43-positive inclusions, or dystrophic neurites in the hypothalamus of case N1.

Case N2 (a Japanese man) had a maternal family history of hypersomnia. Frequent napping episodes at school began at age 12 years, followed by the onset of terrifying hypnagogic hallucinations and sleep paralysis. He described the illusion of a robber entering his bedroom, sitting on his face, and preventing him from moving or screaming for help. His first episode of cataplexy was at age 18 years, and attacks occurred with laughter or excitement (such as winning at Mahjong, or when scolding children). He worked in his father's woodworking company, taking 2 naps on weekdays, and was diagnosed with narcolepsy at age 33 years. His initial 1 nap PSG showed shortened sleep and REM latencies (SL 2 minutes, REML 2 minutes), which were also consistently seen in follow-up 1 nap PSG studies later in his life. After age 70 years, he sometimes stood still or moved during the night while half asleep. His nocturnal PSG at age 72 years showed mild sleep disturbances with an apnea hypopnea index of 9.8, a PLM index of 5.8, and a 7.5-minute stage-1 REM period. At age 74 years, he underwent surgery for bile duct metastasis of testicular carcinoma followed by hormone therapy. He subsequently became anxious and entered a disoriented, agitated, and confusional state at night. Brain MRI at age 74 years revealed age-related mild brain atrophy, but cognitive function was not assessed. He died of spinal cord infarction and sepsis at age 76 years. Neuropathologic examination showed substantial NFT in the neocortex (Braak stage V) and senile plaques in precentral gyrus (Braak stage C, CERAD age-related plaque score C). Neuropathologic diagnosis for AD was CERAD NP possible b.<sup>14</sup> In hypothalamic tissues, several ubiquitin-positive threads and abundant neuropil threads and NFT were observed, mainly in the ventral or medial parts of the posterior hypothalamus including the tuberomammillary nucleus, which is consistent with previous reports showing regional preference of NFT

**Figure 1 Ubiquitin and hypocretin immunoreactivity in hypothalamic tissue of narcolepsy and control subjects**



hypothalamic tissues. Note that hypocretin cell were reduced in narcolepsy (B) vs control (A), and no ubiquitinated inclusions were observed in hypocretin cells in narcolepsy or control (C, D). Scale bar = 1 mm in A and B, 50  $\mu$ m in C and D. Fx = fornix; 3V = third ventricle. Dashed rectangle indicates approximate area used for higher magnification.

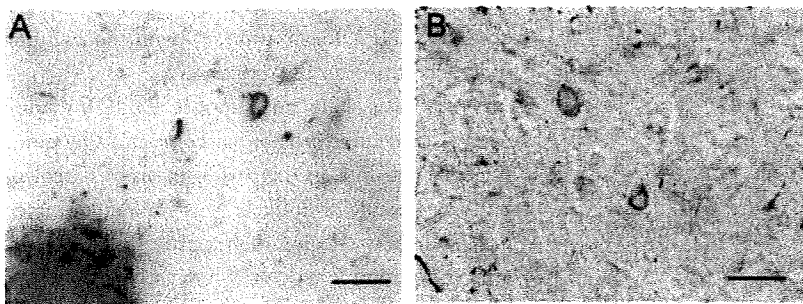
pathology in the hypothalamus.<sup>21</sup> No ubiquitin-positive inclusions were found in the lateral hypothalamic area or in 53 remaining hypocretin cells. There were no amyloid  $\beta$ -positive senile plaques,  $\alpha$ -synuclein-positive inclusions, Lewy neurites, TDP-43-positive inclusions, or dystrophic neurites in the hypothalamus of case N2.

Detailed clinical data of case N3 (a white woman) were not available. Her narcolepsy symptoms of excessive daytime sleepiness and typical cataplexy started in her 20s, and she was diagnosed with narcolepsy. Her nocturnal PSG and Multiple Sleep Latency Test results met International Classification of Sleep Disorders 1 narcolepsy criteria. She had comorbid dementia later in her life, and died of dementia at age 89 years. Immunohistochemical examination revealed many tau-positive NFTs and neuropil threads (Braak stage V) and moderate amounts of senile plaques in the neocortex (CERAD age-related plaque score B). Abundant  $\alpha$ -synuclein-positive Lewy neurites and Lewy bodies were also found in the neocortex. The neuropathologic diagnosis was Lewy body disease. No ubiquitinated in-

clusions were found in the lateral hypothalamic area or in 7 remaining hypocretin cells. Several NFTs and neuropil threads and many Lewy neurites were observed in the ventral part of the posterior hypothalamus. There were no senile plaques,  $\alpha$ -synuclein-positive inclusions, TDP-43-positive inclusions, or dystrophic neurites in the hypothalamus of case N3.

Case N4 (a Japanese woman) began to experience excessive daytime sleepiness at age 10 years. She fell asleep during walking and eating, awakening refreshed after 5-minute naps. Her first episode of cataplexy was at age 13 years, when she experienced sudden loss of muscle tone in her shoulders and knees after a sensation of swelling pride. Hypnagogic hallucinations and sleep paralysis began around the same time, and she described feeling as if she was being crushed by a dead body. She did not realize she was affected by hypersomnia, but was diagnosed with narcolepsy at age 55 years upon her first visit to a hospital. Her initial 1 nap PSG test showed shortened sleep and REM latencies with SOREMP (SL 3 minutes and REML 4 minutes). A resting finger tremor and memory disturbance started at age 72

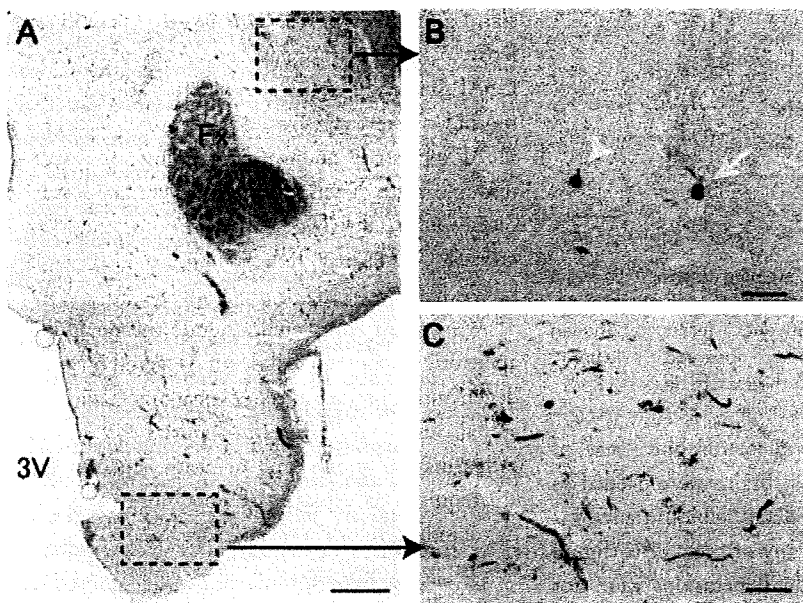
**Figure 2** Ubiquitin-positive inclusions in the cortex of narcolepsy subjects with comorbid dementia



Ubiquitinated inclusions (arrows) were frequently observed in the cortex of narcolepsy patients with comorbid dementia (A; case N2; B; case N3). Scale bar = 50  $\mu$ m.

years, preventing her from taking medicines appropriately. Occasional delirium at night began at age 73 years, and memory disturbances, delusions, and hallucinations in a disoriented state became progressively worse. Brain MRI at age 76 years showed marked brain atrophy in frontal and temporal lobes. Incontinence occurred at age 78 years, and she was restricted to her bed. She died of acute aggravation of chronic renal failure, heart failure, and disseminated intravascular coagulation at age 79 years. Upon neuropathologic examination, massive NFTs and neurofibrillary threads were observed in the subiculum and entorhinal cortex, with some also in neocortex. A few

**Figure 3** Preferential localization of tau-positive NFTs in hypothalamus of narcolepsy subject with comorbid dementia



Tau-positive threads and neurofibrillary tangles (NFTs) (brown) in hypothalamus were preferentially localized in ventral part (C) and sparse in perifornical hypocretin area (B) of narcolepsy with comorbid dementia (case N2). Only 1 NFT (arrow) was found near remaining hypocretin cell (purple; arrowhead). Note that the hypocretin cell had no tau-positive inclusions (B). Scale bar = 1 mm in A, 100  $\mu$ m in B and C. Fx = fornix; 3V = third ventricle.

senile plaques were observed selectively in the hippocampus but not in other cortical regions. Multiple small, old infarctions were found in basal ganglia. The neuropathologic diagnosis was senile dementia of the NFT type.<sup>22</sup> No ubiquitin-positive inclusions were found in the lateral hypothalamic area or in 20 remaining hypocretin cells. A few ubiquitin-positive threads and several tau-positive neurofibrillary threads were observed, mainly in the ventral part of the posterior hypothalamus at the premammillary level, and 1 NFT was found in the tuberomammillary nucleus, which is consistent with a previous report.<sup>21</sup> There were no senile plaques, Lewy neuritis,  $\alpha$ -synuclein-positive inclusions, TDP-43-positive inclusions, or dystrophic neurites in the hypothalamus of case N4.

**Summary of clinical and neuropathologic findings.** All 4 patients had typical narcolepsy, showing cataplexy and SOREMPs, and all carried the HLA-DQB1\*0602 allele (HLA typed at clinic or postmortem). Similar to previous reports, a dramatic ( $\geq 90\%$ ) hypocretin cell loss was observed in all 4 narcolepsy brains examined, indicating that our subjects all had typical narcolepsy with hypocretin deficiency (figure 1).

Three of the 4 patients had comorbid dementia processes on neuropathologic examination. Many ubiquitin-positive inclusions were observed in the cortex of these subjects (figure 2), but no ubiquitinated inclusions were found in cytoplasm or nucleus of hypocretin cells in narcolepsy (regardless of comorbid dementia) (figure 1D) or in control subjects (figure 1C).

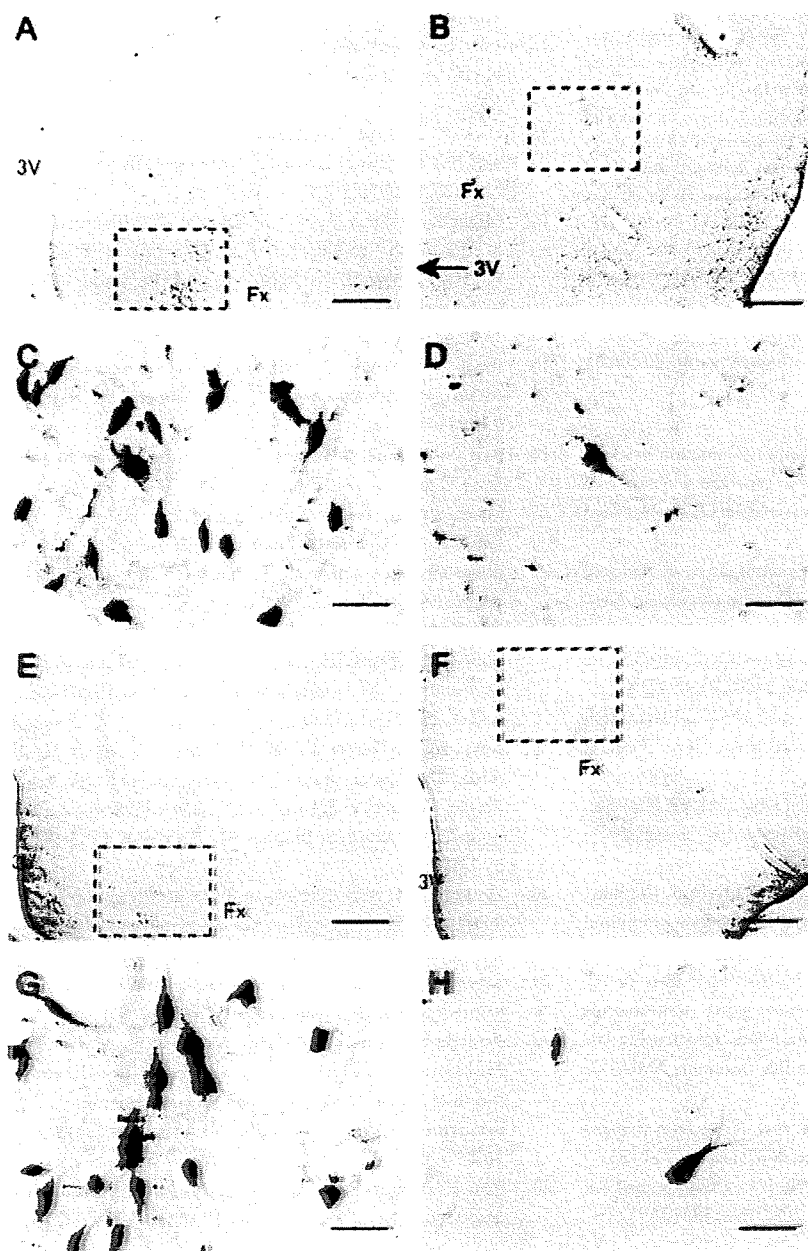
Examination of hypothalamic sections for possible protein aggregates (tau,  $\alpha$ -synuclein, amyloid  $\beta$ , and TDP-43) revealed that all narcolepsy cases had tau-positive NFTs and neurofibrillary threads, showing regional preference, many in the ventral part of the posterior hypothalamus (figure 3C) but sparse in the perifornical hypocretin area (figure 3B).  $\alpha$ -Synuclein-positive Lewy neurites were also observed (case N3). Double immunostaining for tau and ubiquitin, or for  $\alpha$ -synuclein and ubiquitin revealed that part of these tau-positive or  $\alpha$ -synuclein-positive structures were also positive for ubiquitin. No inclusions consisting of these components were observed in hypocretin cells of subjects with narcolepsy (figure 3B).

No differences between narcolepsy and control subjects were observed for glial response markers AIF1 (figure 4, A–D) and GFAP (figure 4, E–H) in the perifornical hypothalamic area.

**DISCUSSION** The presence of ubiquitinated protein aggregates is a hallmark of neurodegenerative diseases.<sup>23</sup> In this study, we used ubiquitin immunoreactivity as a marker to identify putative narcolepsy-specific protein aggregates. Because narcolepsy is



**Figure 4** No increased inflammation markers in hypothalamic hypocretin area of patients with narcolepsy



A microglial activation marker allograft inflammatory factor 1 staining (brown; A-D) and a reactive astrocytic marker glial fibrillary acidic protein staining (brown; E-H) in lateral hypothalamic area were stained with hypocretin (purple). No significant differences between control (A, C, E, G; case C1) and narcolepsy (B, D, F, H; case N2) were observed. Scale bar = 1 mm in A, B, E, and F; 50  $\mu$ m in C, D, G, and H. Fx = fornix; 3V = third ventricle.

associated with nearly complete disappearance of hypocretin cells, 4 narcolepsy brains were needed to study 96 hypocretin cells in detail. Ubiquitinated inclusions were not found in any of these cells (figure 1). Interestingly, ubiquitinated inclusions were not found in hypocretin cells in 3 of 4 narcolepsy patients with comorbid dementia. The few ubiquitin-positive granular or dot-like structures observed (figure 1) may be associated with aging, as previously reported.<sup>5</sup> Additional screening of known protein ag-

gregates showed that tau-positive NFTs were observed mainly in ventral part of posterior hypothalamus and scarcely in the perifornical hypocretin area (figure 3), confirming a previous report describing NFT localization.<sup>21</sup> Again, no inclusions in hypocretin neurons were observed.

Our findings do not support a role for known neurodegenerative processes accompanied by ubiquitinated inclusions in the pathogenesis of narcolepsy, but it is possible, if unlikely, that the remaining cells have somehow escaped such a process. Indeed, protein aggregation is suggested to be a protective cellular response<sup>23</sup> rather than a cause of degeneration. In this context, the failure to form ubiquitinated inclusions could reflect an increased vulnerability of hypocretin cells to yet unknown pathologic process. Nevertheless, the majority of hypocretin cells lost in narcolepsy could not involve ubiquitinated inclusions demonstrated by few ubiquitinated inclusions in the perifornical hypocretin area.

Our study of AIF1 and GFAP immunoreactivity in the perifornical area also found no active inflammation (microglial response) or residual gliosis (astrocytic fibrous network), extending our preliminary findings in a small number of subjects using HLA-DR and GFAP.<sup>1</sup> These findings are compatible with the lack of ubiquitinated protein aggregation in remaining hypocretin cells, which would have caused inflammation along with progressive neurodegeneration. These findings are also compatible with the nonprogressive clinical course of most narcolepsy cases, i.e., rapid onset and stable symptomatology. Controversy exists regarding the increase of GFAP staining in the hypothalamus of subjects with narcolepsy.<sup>1,2</sup> In this study, we observed no increase in GFAP staining even in narcolepsy patients with comorbid dementia. Astrocytic activation with reactive GFAP increase is a nonspecific finding associated with multiple forms of neuronal injury, including subclinical cases. Our results suggest that previous reports of increased GFAP may reflect interindividual variance rather than narcolepsy neuropathology.

We cannot completely exclude the possibility of apoptotic hypocretin cell death triggered by a neurodegenerative process at narcolepsy onset, with no residual abnormal protein deposits or traces of inflammation at the time of death. Further studies are required to explore the possibility of apoptotic hypocretin cell loss in narcolepsy.

#### ACKNOWLEDGMENT

The authors thank Ms. Mali Einen at Stanford University for clinical coordination; the Stanford Brain Bank for providing brain samples; Drs. Shuji Iritani, Kazuhiro Niizato, and Ken-ichi Oshima at the Tokyo Metropolitan Matsuzawa Hospital for conducting autopsies; and Dr. Juliette Faraco for critical reading and editing.

## DISCLOSURE

Dr. M. Honda receives research support from the Ministry of Education, Science and Culture of Japan [Grants-in-Aid for Scientific Research: 17390324 (PI) and 19390310 (PI); Priority Areas "Comprehensive Genomics" (Collaborative researcher)]. Dr. Arai reports no disclosures. Dr. Fukazawa reports no disclosures. Dr. Y. Honda receives research support from the Ministry of Education, Science and Culture of Japan [Grant-in-Aid for Scientific Research: 18603013 (PI)]. Dr. Tsuchiya reports no disclosures. Dr. Salehi has applied for a patent at Stanford's Office of Technology Transfer related to the treatment of Down syndrome and receives research support from the Alzheimer Association Thrasher Foundation. Dr. Akiyama reports no disclosures. Dr. Mignot receives research support from the NIH [23724 (PI), MH080957 (PI), and NS062798 (PI)]. He is also funded by the Howard Hughes Medical Institute and has received research gifts from Respiration, Cephalon, Resmed, Elli Lilly, and Jazz Pharmaceuticals.

Received January 27, 2009. Accepted in final form May 1, 2009.

## REFERENCES

1. Peyron C, Faraco J, Rogers W, et al. A mutation in a case of early onset narcolepsy and a generalized absence of hypocretin peptides in human narcoleptic brains. *Nat Med* 2000;6:991-997.
2. Thannickal TC, Moore RY, Nienhuis R, et al. Reduced number of hypocretin neurons in human narcolepsy. *Neuron* 2000;27:469-474.
3. van den Pol AN. Narcolepsy: a neurodegenerative disease of the hypocretin system? *Neuron* 2000;27:415-418.
4. Scammell TE. The frustrating and mostly fruitless search for an autoimmune cause of narcolepsy. *Sleep* 2006;29:601-602.
5. Gray DA, Tsigiotis M, Woulfe J. Ubiquitin, proteasomes, and the aging brain. *Sci Aging Knowledge Environ* 2003;2003:RE6.
6. Neumann M, Sampathu DM, Kwong LK, et al. Ubiquitinated TDP-43 in frontotemporal lobar degeneration and amyotrophic lateral sclerosis. *Science* 2006;314:130-133.
7. Arai T, Hasegawa M, Akiyama H, et al. TDP-43 is a component of ubiquitin-positive tau-negative inclusions in frontotemporal lobar degeneration and amyotrophic lateral sclerosis. *Biochem Biophys Res Commun* 2006;351:602-611.
8. Fronczek R, Overeem S, Lee SY, et al. Hypocretin (orexin) loss in Parkinson's disease. *Brain* 2007;130:1577-1585.
9. Thannickal TC, Lai YY, Siegel JM. Hypocretin (orexin) cell loss in Parkinson's disease. *Brain* 2007;130:1586-1595.
10. Benarroch EE, Schmeichel AM, Sandroni P, Low PA, Parisi JE. Involvement of hypocretin neurons in multiple system atrophy. *Acta Neuropathol* 2007;113:75-80.
11. Petersen A, Gil J, Maat-Schieman ML, et al. Orexin loss in Huntington's disease. *Hum Mol Genet* 2005;14:39-47.
12. Love S, Bridges LR, Case CP. Neurofibrillary tangles in Niemann-Pick disease type C. *Brain* 1995;118(pt 1):119-129.
13. Crocker A, Espana RA, Papadopoulou M, et al. Concomitant loss of dynorphin, NARP, and orexin in narcolepsy. *Neurology* 2005;65:1184-1188.
14. Mirra SS, Heyman A, McKeel D, et al. The Consortium to Establish a Registry for Alzheimer's Disease (CERAD), part II: standardization of the neuropathologic assessment of Alzheimer's disease. *Neurology* 1991;41:479-486.
15. Braak H, Braak E. Neuropathological staging of Alzheimer-related changes. *Acta Neuropathol* 1991;82:239-259.
16. Mai JK, Assheuer J, Paxinos G. Atlas of the Human Brain. San Diego: Academic Press; 1997.
17. Hasegawa M, Jakes R, Crowther RA, Lee VM, Ihara Y, Goedert M. Characterization of mAb AP422, a novel phosphorylation-dependent monoclonal antibody against tau protein. *FEBS Lett* 1996;384:25-30.
18. Obi K, Akiyama H, Kondo H, et al. Relationship of phosphorylated alpha-synuclein and tau accumulation to Abeta deposition in the cerebral cortex of dementia with Lewy bodies. *Exp Neurol* 2008;210:409-420.
19. Kametani F, Tanaka K, Ishii T, Ikeda S, Kennedy HE, Allsop D. Secretory form of Alzheimer amyloid precursor protein 695 in human brain lacks beta/A4 amyloid immunoreactivity. *Biochem Biophys Res Commun* 1993;191:392-398.
20. Hasegawa M, Arai T, Nonaka T, et al. Phosphorylated TDP-43 in frontotemporal lobar degeneration and amyotrophic lateral sclerosis. *Ann Neurol* 2008;64:60-70.
21. Saper CB, German DC. Hypothalamic pathology in Alzheimer's disease. *Neurosci Lett* 1987;74:364-370.
22. Yamada M, Itoh Y, Otomo E, Suematsu N, Masushita M. Dementia of the Alzheimer type and related dementias in the aged: DAT subgroups and senile dementia of the neurofibrillary tangle type. *Neuropathology* 1996;16:89-98.
23. Ross CA, Poirier MA. Protein aggregation and neurodegenerative disease. *Nat Med* 2004;10(suppl):S10-S17.

## TDP-43 pathology in familial British dementia

Claudia Schwab · Tetsuaki Arai · Masato Hasegawa ·  
Haruhiko Akiyama · Sheng Yu · Patrick L. McGeer

Received: 12 February 2009 / Revised: 13 February 2009 / Accepted: 3 March 2009 / Published online: 13 March 2009  
© Springer-Verlag 2009

**Abstract** Trans-activation-responsive DNA-binding protein 43 (TDP-43) is a component of pathological inclusions in amyotrophic lateral sclerosis and several forms of sporadic and familial frontotemporal lobar degeneration. This has suggested defining a new class of diseases known as TDP-43 proteinopathies. However, it has been reported more recently that TDP-43 positive inclusions occur in other neurodegenerative disorders such as Alzheimer's disease, Dementia with Lewy Bodies and Parkinsonism dementia complex of Guam. Here we report the occurrence of TDP-43 inclusions in one other neurodegenerative disorder: familial British dementia. Using a variety of antibodies against phosphorylated and non-phosphorylated TDP-43 epitopes, we found intense accumulation occurred in the form of dystrophic neurites, neuronal cytoplasmic inclusions and was also occasionally associated with neurofibrillary tangles. Double immunostaining revealed that TDP-43 and tau aggregates were rarely directly colocalized, but

co-existed in the same neurons as separate inclusions. Double staining with ubiquitin showed a direct colocalization with TDP-43. The phosphorylation-dependent TDP-43 antibodies proved superior to phosphorylation-independent antibodies in revealing pathological inclusions since the former did not stain non-phosphorylated TDP-43 in normal nuclei. Our results support the concept that TDP-43 pathology is not narrowly restricted, but is involved in the etiology of many neurodegenerative disorders.

**Keywords** TDP-43 · Familial British dementia · ABri · Ubiquitin · Intracellular inclusions · Phosphorylation-dependent TDP-43 antibodies

### Introduction

Trans-activation-responsive (TAR) DNA-binding protein 43 (TDP-43) has been identified as a major component of ubiquitinated tau-negative inclusions in several forms of sporadic and familial frontotemporal lobar degeneration (FTLD) and amyotrophic lateral sclerosis (ALS) [2, 25]. For this common trait, these disorders were grouped together as a new entity of neurodegenerative diseases, TDP-43 proteinopathies [6, 20]. TDP-43 is ubiquitously expressed and involved in regulating transcription and alternative splicing [4, 5, 26]. TDP-43 has also been linked to cytoskeletal stability and axonal transport by a recent study, which showed that TDP-43 regulates hNFL RNA stability [32].

More recently an association of TDP-43 with other inclusion-forming proteins has been described. TDP-43 inclusions have been shown to co-exist with tau aggregates in a subset of Alzheimer's disease (AD) cases, particularly those with hippocampal sclerosis [1, 3, 13, 15, 22, 33],

---

C. Schwab · S. Yu · P. L. McGeer (✉)  
Department of Psychiatry, Kinsmen Laboratory of Neurological Research, University of British Columbia, 2255 Wesbrook Mall, Vancouver, BC V6T 1Z3, Canada  
e-mail: mcgeerpl@interchange.ubc.ca

C. Schwab  
e-mail: cschwab@cmmt.ubc.ca

T. Arai · H. Akiyama  
Department of Psychogeriatrics, Tokyo Institute of Psychiatry, Tokyo Metropolitan Organization for Medical Research, 2-1-8 Kamikitazawa, Setagaya-ku, Tokyo 156-8585, Japan

M. Hasegawa  
Department of Molecular Neurobiology, Tokyo Institute of Psychiatry, Tokyo Metropolitan Organization for Medical Research, 2-1-8 Kamikitazawa, Setagaya-ku, Tokyo 156-8585, Japan



Parkinsonism dementia complex of Guam (PDC-G) [9, 11, 21] as well as argyrophilic grain disease (AGD) [8] and coexistence with tau deposits also occurs in some cases of Pick's disease and corticobasal degeneration [7, 13, 33]. Association with alpha-synuclein containing inclusions has been described in Lewy body dementia (LBD) and Parkinson's disease (PD) [3, 13, 22]. Additionally we recently reported colocalization of TDP-43 with huntingtin inclusions in Huntington's disease (HD) [30].

Familial British dementia (FBD) is another neurodegenerative disorder characterized by tau inclusions and amyloid deposits. While tau aggregates similarly to the neurofibrillary tangles (NFT) in AD, the amyloid plaques in FBD are created by ABri, and not by  $\beta$ -amyloid of AD, and the distribution of plaques is different to that of AD.

Familial British dementia is a rare familial disorder caused by a point mutation in the *BRI* gene [34]. This mutation changes a stop-codon and leads to an 11-amino acid extension of Bri-precursor protein. Its 22 C-terminal amino acids are cleaved off as ABri peptide and aggregate in the form of various types of amyloid plaques and angiopathy [14]. The deposition of the amyloidogenic ABri is accompanied by tau pathology, in the form of AD-type NFT, dystrophic neurites (DN) and neuropil threads [10, 28, 35].

ABri amyloid deposition in FBD is generally limited to the limbic system, the cerebellum and brain stem areas. Tau pathology is found in the same regions, except the cerebellum [14].

Since association of TDP-43 with tau aggregates has been reported in AD and PDC-G [1, 9, 11, 13, 22, 33], we examined if such an association also exists in FBD and whether the distribution of TDP-43 pathology correlates with that of ABri amyloid and tau aggregates.

## Materials and methods

For this study the following cases were selected from our brain bank at the University of British Columbia: one case of familial British dementia (female, 64 years, postmortem delay 4 h) and two elderly control cases (female, 87 years, 4 h postmortem delay and male, 72 years, 4.5 h postmortem delay). The FBD case had been identified in a family described by Plant and colleagues [28] and appears as V44 in Fig. 1.

Immunohistochemistry was carried out on brain tissue using a panel of antibodies against TDP-43, tau, ubiquitin,  $\beta$ -amyloid and ABri. Their source and dilutions used are

**Fig. 1** Photomicrographs of immunohistochemistry in amygdala (a–d), CA1 (e–h), entorhinal cortex (i–l), midtemporal cortex (m–p) and cerebellum (q–t) of a case with familial British dementia. The first column (a, e, i, m, q) shows that ABri-labeled deposits appear in all regions except midtemporal cortex, where only amyloid angiopathy is found. Abnormal tau inclusions are most dense in amygdala and entorhinal cortex (b, j), a moderate number is found in CA1 and midtemporal cortex (f, n), and none in the cerebellum (r). Distribution of ubiquitin is similar (c, k, o, s), with the exception of CA1 where many extracellular NFTs are stained (g). Immunostaining of TDP-43 parallels that of tau (d, h, l, p, t). Calibration bar 100  $\mu$ m, except in a–d and i–l: 50  $\mu$ m

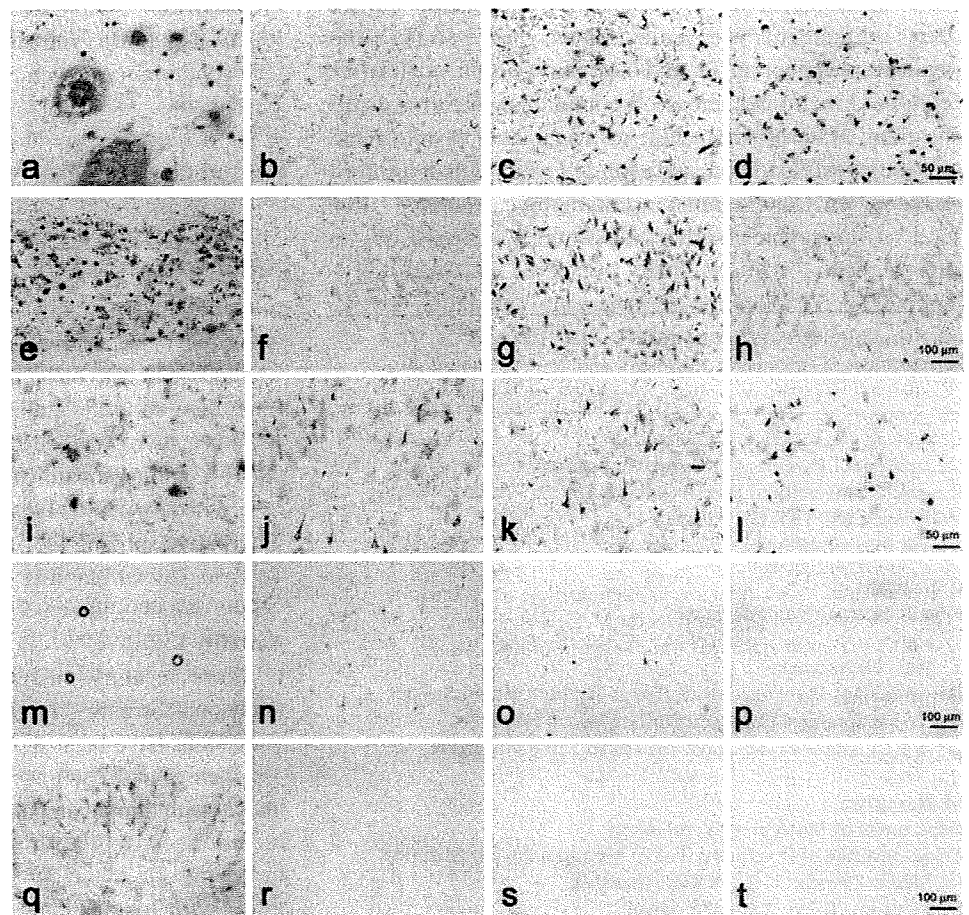


**Table 1** Antibody source and dilutions

Antibody	Source	Catalog #	Antigen/specificity	Host, dilution (DAB/fluorescence)
AT8	Pierce, Rockford, IL	MN1020	PHF tau pS202	Mouse, 1:3,000/1:500
A0024	Dako, Carpinteria, CA	A0024	C-term. of recombinant human tau	Rabbit, 1:2,000/1:1000
ABri	Dr. H. Akiyama <sup>a</sup> [31]	NA	ABri 22-34	Rabbit, 1:10,000/1:5,000
6F3D	DAKO, Mississauga, ON	M0872	Synthetic $\beta$ -amyloid, 8-17	Mouse, 1:500/ND
Ubiquitin	DAKO, Mississauga, ON	Z0458	Ubiquitin from cow erythrocytes	Rabbit, 1:1,000/1:200
TDP-43	ProteinTech, Chicago, IL	10782-2-AP	Recombinant protein	Rabbit, 1:300/ND
TDP-43	Abnova, Taipei, Taiwan	H00023435-A01	Full-length recombinant protein with GST tag (1-261)	Mouse, <sup>b</sup> 1:300/200
TDP-43 pS403/04	Dr. M. Hasegawa <sup>a</sup> [12]	NA	TDP-43 (398-408, pS403/404)	Rabbit, 1:2,000/1:1,000
TDP-43 pS409/10	Dr. M. Hasegawa <sup>a</sup> [12]	NA	TDP-43 (405-414, pS409/410)	Rabbit, 1:2,000/ND
TDP-43 pS409/10 (m)	Dr. M. Hasegawa <sup>a</sup> [17]	NA	TDP-43 (405-414, pS409/410)	Mouse, <sup>b</sup> 1:5,000/1:1,000
Anti-TDP-43N (3-12)	Dr. M. Hasegawa <sup>a</sup>	NA	TDP-43 (N-terminal)	Rabbit, <sup>b</sup> 1:5,000/ND
Anti-TDP-43C (405-414)	Dr. M. Hasegawa <sup>a</sup> [12]	NA	TDP-43 (C-terminal)	Rabbit, 1:5,000/ND

<sup>a</sup> Tokyo Institute of Psychiatry, Tokyo, Japan

<sup>b</sup> Antigen retrieval

ND Not determined, NA not applicable

shown in Table 1. The phosphorylated TDP-43 antibodies were raised against phosphorylated sequences of human TDP-43 [12, 17] and have the advantage of not recognizing normal TDP-43.

Brain tissues had been fixed in 4% paraformaldehyde, and, after 3–4 days, transferred to a 15% buffered sucrose maintenance solution. For immunohistochemistry, 30  $\mu$ m sections of selected brain areas were cut on a freezing microtome (American Optical Corporation, Buffalo, NY).

For light microscope immunostaining, the sections were treated for 30 min with 0.5% H<sub>2</sub>O<sub>2</sub> solution in 0.01 M phosphate buffered saline, pH 7.4, containing 0.3% Triton X-100 (PBS-T), transferred into 5% skim milk in PBS-T for 30 min, and incubated for 72 h at 4°C or overnight at room temperature with one of the primary antibodies (Table 1). Sections were next treated with the appropriate biotinylated secondary antibodies (DAKO, Mississauga, ON, 1:2,000) for 2 h at room temperature, followed by incubation in avidin–biotinylated horseradish peroxidase complex (DAKO, Mississauga, ON, 1:10,000) for 1 h at room temperature. Peroxidase labeling was visualized by incubation in 0.01% 3,3-diaminobenzidine (DAB; Sigma, Oakville, ON) containing 1% nickel ammonium sulfate (Fisher Scientific, Ottawa, ON), 5 mM imidazole (BDH Laboratory Supplies, Poole, UK) and 0.001% H<sub>2</sub>O<sub>2</sub> in 0.05 M Tris–HCl buffer, pH 7.6. When a dark purple/black color developed, sections were washed, mounted on glass slides, air-dried, and coverslipped with Entellan (EMD Biosciences, Gibbstown, NJ). Some sections were counterstained with Neutral Red (BDH Laboratory Supplies, Poole, UK) prior to coverslipping. Antigen retrieval as indicated in Table 1 was carried out by boiling the sections in

PBS for 5 min prior to all other steps to improve the staining of inclusions.

For double immunofluorescence staining, sections were incubated in 5% skim milk in PBS-T for 30 min, and then incubated for 72 h at 4°C or overnight at room temperature with a combination of two primary antibodies. These combinations were: AT8/TDP-43(pS403/404), A0024/TDP-43(Abnova), TDP-43(mouse pS409/10)/ABri 1129 and TDP-43(mouse pS409/10)/Ubiquitin (for the source and concentration of antibodies used see Table 1). Sections were next incubated with a mixture of fluorophore-labeled secondary antibodies (Alexa Fluor 488 goat-anti-mouse and Alexa Fluor 546 goat-anti-rabbit, Invitrogen, Burlington, ON, Canada; 1:500) in the dark, counterstained with Hoechst 33258 (Invitrogen, Burlington, ON, Canada), and mounted on glass slides. To reduce lipofuscin autofluorescence, sections were next treated with a solution of 0.3% Sudan Black B (Gurr Ltd, London, UK) in 70% ethanol for 7 min and washed in PBS eight times [29]. Subsequently, sections were air-dried and coverslipped with Prolong Gold (Invitrogen, Burlington, ON). The staining pattern for each individual antibody following the double-fluorescence staining was identical to the pattern observed in single immunostaining experiments. Controls for immunostaining were performed by omitting the primary antibodies. No staining was observed in these controls.

Confocal images were captured with a spindisk confocal microscope (inverted Olympus widefield microscope with Carv Spindisk, Olympus, Center Valley, PA) at 60 $\times$  objective magnification. Fluorescent images were colocalized with ImagePro software (Improvision Inc., Waltham, MA). To assist interpretation of the figures, TDP-43 antibodies

were always assigned the color green and tau, ABri and ubiquitin antibodies were assigned the color red in the false color assignment with ImagePro.

## Results

In the control cases, no immunostaining was found with the antibodies against ABri (ABri 1129) or with the phosphorylation-dependent antibodies against TDP-43 (TDP-43 pS403/04, TDP-43 pS409/10, mouse TDP-43 pS409/10). The phosphorylation-independent TDP-43 antibodies stained nuclei of neurons and glia cells. The antibodies against tau and ubiquitin revealed occasional DNs and NFTs in hippocampus, fusiform and temporal cortex.

The results of immunostaining with the ABri, tau, TDP-43 and ubiquitin antibodies in the FBD case are summarized in Table 2.

The ABri antibody stained various types of amyloid deposits in the form of diffuse, compact and star-shaped plaques and vessel associated amyloid angiopathy (Fig. 1 first column, Fig. 3r). These deposits were most frequently found in the hippocampus, entorhinal cortex and cerebellum, although the cerebellum was devoid of compact and star-shaped plaques. The other areas examined contained amyloid angiopathy and only minor diffuse amyloid deposits. No staining was found with the 6F3D antibody against  $\beta$ -amyloid in the FBD case.

Pathological patterns revealed by the *tau antibodies* (AT8 and A0024) included numerous intracellular NFTs (iNFTs), pre-tangle neurons and a thick meshwork of DNs and neuropil threads (Fig. 1, column 2). These inclusions were most densely distributed throughout the amygdala and the entorhinal cortex. Many dentate granule neurons had tau-positive inclusions. Hippocampal CA1 and subiculum were almost devoid of surviving neurons but contained many extracellular NFTs (eNFTs). Therefore, very few iNFTs were present in these regions and stained by the tau antibodies. However, thick, elongated dystrophic neurites were frequently associated with the eNFT forming tangle associated neuritic clusters (TANCs). In brainstem regions, such as the locus coeruleus, periaqueductal gray and thalamus, tau pathology in the form of iNFTs was less frequent. The cerebellum was devoid of tau pathology.

The *ubiquitin antibody* stained a dense network of DNs, neuronal cytoplasmic inclusions (NCIs) and NFTs (Fig. 1 column 3). Distribution and extend of staining was similar to that observed with the tau antibodies. But while the tau antibodies labeled a dense web of DNs and neuropil threads of various calibers, mostly thick elongated DNs were labeled by the ubiquitin antibody. Additionally to the above described pattern, Marinesco bodies in the SN were labeled only by the ubiquitin antibody.

The staining patterns with the three phosphorylation-dependent *TDP-43 antibodies* were very similar, labeling NCIs, DNs, and single fiber strands in iNFTs (Fig. 2). This

**Table 2** Pathological pattern in FBD

Brain region	ABri		Tau		TDP-43		Ubi	
	Severity	Pattern	Severity	Pattern	Severity	Pattern	Severity	Pattern
Amygdala	++++	dPl, cPl, AA, IG	++++	iNFT, preNFT, DN, NPT, TANC	+++	NCI, iNFT, DN, TANC	++++	iNFT, eNFT, NCI, DN, TANC
CA1/subiculum	++++	dPl, cPl, AA, IG	+	DN, NPT, TANC	+	DN, TANC	++	iNFT, eNFT, DN
Dentate gyrus	++	dPl, cPl	+++	PreNFT, DN	+	NCI, DN	++	NCI, DN
Entorhinal cortex	+++	dPl, cPl, AA, IG	+++	iNFT, preNFT, DN, NPT, TANC	++	NCI, iNFT, DN, TANC	+++	iNFT, eNFT, NCI, DN, TANC
Midfrontal cortex	+	AA	+	DN	–		±	DN
Temporal cortex	++	dPl, AA	+	iNFT, DN, NPT	–		+	iNFT, DN
Supramarginal cortex	+	dPl, AA	–		–		–	
Visual cortex	+	AA	–		–		–	
Thalamus	+	dPl, AA	+	iNFT	+	DN	+	iNFT, DN
Locus coeruleus	+++	dPl, AA	+	iNFT	–		+	iNFT, DN
Substantia nigra	–		–		–		±	DN, Marinesco B
Periaqueductal gray	+++	dPl, AA	+	iNFT	–		+	iNFT, DN
Pedunculi cerebri	++	dPl, AA	–		–		–	
Cerebellum	++++	dPl, AA	–		–		–	

*Ubi* Ubiquitin, *dPl* diffuse plaques, *cPl* compact plaques, *AA* amyloid angiopathy, *IG* intracellular glial aggregates, *iNFT* intracellular neurofibrillary tangles, *preNFT* pre-tangle neurons, *DN* dystrophic neurites, *NPT* neuropil threads, *TANC* tangle associated neuritic clusters, *NCI* neuronal cytoplasmic inclusions

TDP-43 pathology was predominantly found in the gray matter. Dystrophic neurites were mostly of a large caliber in various shapes and sizes, forming round and elongated hooks and loops. Spherical dystrophic neurites were associated with extracellular NFTs (TANCs). NCI's were of various sizes and shapes. Some neurons contained merely a few wisps of TDP-43 immunopositive material, others were filled with a dense cocoon-like net and some contained solid inclusions filling almost the entire perikaryon. The C-terminal and phosphorylation-dependent TDP-43 antibodies also labeled peculiar starfish-shaped inclusions (Fig. 2p, q). Intranuclear TDP-43 aggregates were not found. The distribution of TDP-43 inclusions paralleled that of pathological tau immunoreactivity. Intense pathology was present in the amygdala and the entorhinal cortex. Moderate pathology was present in the adjacent fusiform gyrus, the dentate gyrus, CA1 and subiculum and light pathology was present in brainstem and some isocortical regions. No TDP-43 pathology was found in the cerebellum (Fig. 1t). In the amygdala and CA1, the density of TDP-43 inclusions was similar to that of the tau inclusions, but it was lower in all other areas examined. While the staining density of the C-terminal phosphorylation-independent TDP-43 antibody was comparable to that of the phosphorylation-dependent TDP-43 antibodies, the antibody against the N-terminal of TDP-43 stained fewer inclusions (Table 3). In addition to the pathological inclusions, the phosphorylation-independent TDP-43 antibodies labeled normal appearing cell nuclei. In areas with a high load of pathology, this nuclear staining was greatly diminished, as has been described as 'clearing' of nuclei [25].

**TDP-43 and tau.** Confocal microscopy of double-immunostained sections with TDP-43 and tau antibodies, revealed that TDP-43 and tau inclusions often coexisted within the same neurons (Fig. 3). However, the staining was only rarely directly colocalized. Instead, TDP-43 and tau-labeled separate parts of the same inclusions or more often completely separate inclusions in the same neuron. NFT fibers were labeled by the tau antibodies while TDP-43 labeled round inclusions nestled between the tau-positive strands. Exceptions to this separate staining pattern were occasional fibers in tau-immunoreactive NFTs which appeared to be coated with TDP-43 (Fig. 3e–h). In addition to neurons with both TDP-43 and tau-labeled inclusions, many neurons had only one type of inclusion, either positive for TDP-43 or tau. In the amygdala, half of the neurons with any type of inclusion contained both TDP-43 and tau aggregates, while the other half had either TDP-43 or tau inclusions (approximately 25% for each type). Both tau antibodies stained a dense network of dystrophic dendrites and neuropil threads, often obscuring neuronal inclusions. Dystrophic neurites labeled by TDP-43 were more sparse, thicker and contorted. In TANCs, tau and TDP-43 labeled

different sets of DN's. Tau stained DN's were elongated while TDP-43 labeled round DN's. In addition to the pathological aggregates, the monoclonal TDP-43 (Abnova) antibody stained normal appearing nuclei in neurons that carried tau-NFT.

**TDP-43 and ubiquitin.** Almost all TDP-43 immunostained inclusions were also labeled by the ubiquitin antibody (Fig. 3u–x). In contrast to tau, ubiquitin and TDP-43 labeling were directly colocalized. Additionally, the ubiquitin antibody stained many inclusions that were unstained by TDP-43; the majority of these were NFTs and DN's. The number of ubiquitin-labeled DN's was approximately one order of magnitude higher than that of DN's stained by TDP-43. However, a small number of small round DN's was negative for ubiquitin staining and labeled with TDP-43 only. While in the amygdala and the entorhinal cortex the number of neurons containing TDP-43 inclusions was only slightly lower than the number of neurons with ubiquitin inclusions, in other areas like the parahippocampal gyrus and adjacent temporal cortex a much higher proportion was stained with ubiquitin alone.

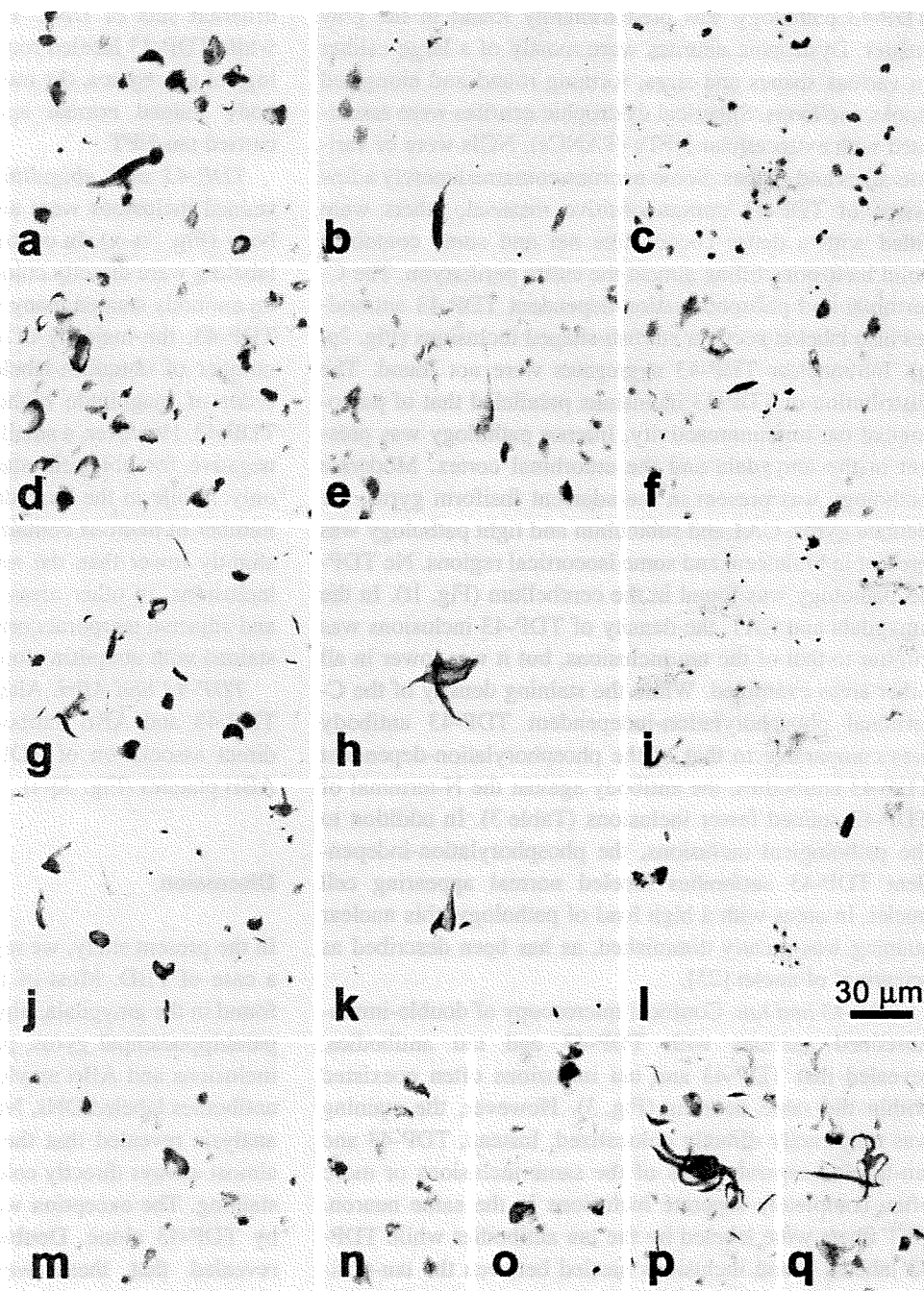
**TDP-43 and ABri.** Although immunostaining with both TDP-43 and ABri antibodies was intense, there was no direct association of TDP-43-labeled DN's or NCI's with ABri plaques (Fig. 3q–t).

## Discussion

In the present study, we report severe TDP-43 pathology in a case of FBD. Most of the pathological inclusions were found in the amygdala, hippocampus, entorhinal cortex and parahippocampal gyrus, paralleling the distribution of tau inclusions and ABri amyloid in this disorder. The TDP-43 antibodies labeled DN's, NCI's and fibers in NFTs. Confocal analysis revealed that the TDP-43 immunoreactivity was almost always directly colocalized with ubiquitin immunostaining. The exception was rare DN's which were stained by TDP-43 alone. Double staining of TDP-43 with tau revealed that these were rarely directly colocalized although many neurons contained both types of inclusions. No immunostaining for  $\beta$ -amyloid was detected, ruling out confounding AD-type pathology.

This report is based on the single case available to us. However, the occurrence of TDP-43 in FBD parallels other reports on conditions where there is co-deposition of TDP-43 with tau. They include AD, PDC-G, AGD and Pick's disease [1, 7–9, 11, 13, 21, 22, 33]. As in these other 'taupathies', TDP-43 in FBD is rarely directly colocalized with tau, but is frequently found as separate inclusions in the same neurons [1, 9, 11, 13]. The rate of TDP-43/tau double-labeling in FBD was higher than reported in AD by Hasegawa and colleagues [11].

**Fig. 2** Immunostaining with various TDP-43 antibodies in FBD at high magnification. Neuronal cytoplasmic inclusions (NCI) and dystrophic neurites (DN) (first column a, d, g, j), fibers in neurofibrillary tangles (NFT) (second column b, e, h, k) and tangle associated neuritic clusters (TANC) (third column c, f, i, l) are stained by all TDP-43 antibodies (a–c: ProteinTech, d–f: Abnova, g–i: pS409-410, j–l: monoclonal pS409-10, m: anti-TDP-43N (3-12). Additionally skein-like (n, Abnova), small ring-shaped (o, Abnova) and starfish-shaped inclusions (p, q; pS403-403) were stained by several of the antibodies. Note that ProteinTech, Abnova and anti-TDP-43N (3-12) antibodies stain normal appearing nuclei in addition to abnormal inclusions and. Sections in d–f and o–q were counterstained with Neutral Red. Calibration bar in l 30  $\mu$ m

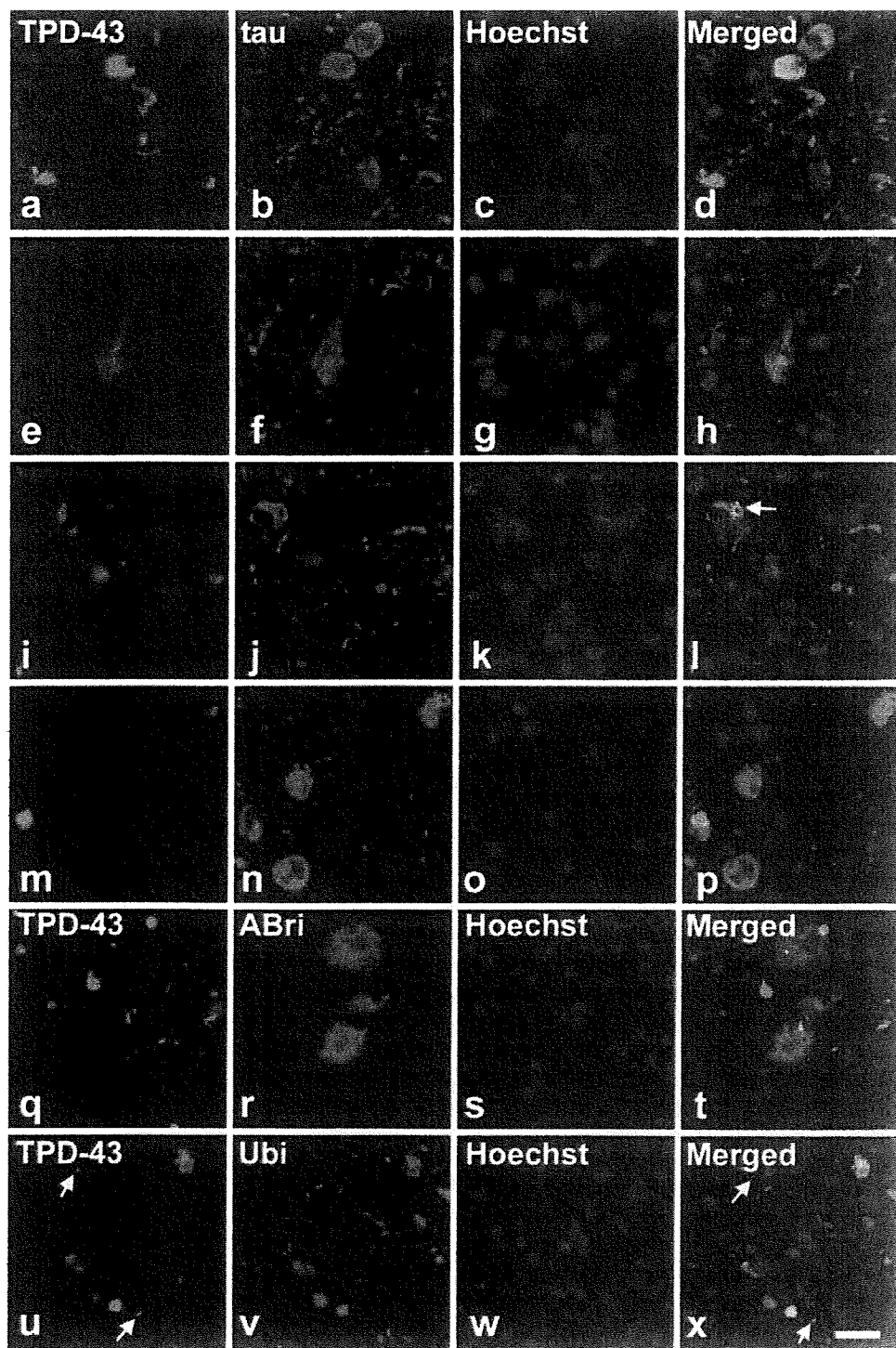


Approximately half of neurons with TDP-43 had also tau inclusions in AD [11], while in the amygdala of FBD, approximately two-thirds of TDP-43 inclusions were accompanied by tau inclusions. This could be explained by differences in the pathoetiology or variations in severity of pathology in the individual cases. Although the selection of brain regions available for this FBD case was limited, most severe pathology was found in the amygdala, indicating that the anatomical pattern and progression of TDP-43 pathology may be similar to the pattern observed in AD and DLB [3, 15].

The types of TDP-43 inclusions found in FBD were NCIs, DNs and occasional fibers in NFTs; similar to the inclusions described in AD and PDC-G [1, 9, 11, 13]. Glial TDP-43 inclusions have been described in PDC-G [9], but were not found in FBD. This parallels reports of prominent glia pathology in PDC-G [21, 27] but not in FBD. Lack of glia pathology in FBD may be the reason for predominance of TDP-43 inclusions in gray matter compared to white matter. In PDC-G the severity of TDP-43 pathology has been described as equal in white and gray matter or even more severe in white matter [9, 11].



**Fig. 3** Confocal images of double staining with TDP-43, tau, ABri and ubiquitin. **a–l** pS 403/404 (green: **a, e, i**) and AT8 (red: **b, f, j**). Sections were counterstained with Hoechst 33258. Tau and TDP-43 inclusions co-exist but are not colocalized (**a–d**). A tau-labeled tangle contains a few TDP-43-labeled fibers (**e–h**). Occasionally tau-NFTs contain small ring-shaped TDP-43 inclusions (**i–l**, arrow). **m–t** TDP-43 Abnova (green: **m**) and A0024 (red: **n**). Although TDP-43 and tau inclusions co-exist in the same neuron, the staining is not directly co-localized (**p**). Double-fluorescence staining of TDP-43 (green: monoclonal pS409/10, **q, u**) with ABri 1129 (red: **r**) or ubiquitin (red: **v**). TDP-43 inclusions are not associated with ABri plaques (**q–t**). Double staining with ubiquitin (**u–x**) reveals that most TDP-43 labeled inclusions are stained by ubiquitin. Several inclusions (possibly NFT) are positive for ubiquitin alone (**v**), and some small DNs are stained by TDP-43 only (**u, x**, arrows). Sections were counterstained with Hoechst 33258. Calibration bar 20  $\mu$ m in **a–p** and 30  $\mu$ m in **q–x**



In contrast to other TDP-43 proteinopathies (ALS and FTLD), in this case of FBD, no TDP-43 containing intranuclear inclusions (NII) were found. Even in most types of FTLD, with the exception of cases with VCP mutations, NII are “never very numerous” [19, 24]. Presence of NII was reported only in a fraction of cases in AD and PDC-G [11, 13] and not found in LBD [22]. Lack of intranuclear

TDP-43 inclusions could indicate differences in the mechanism of the disorders.

In FBD, antibodies which recognize TDP-43 phosphorylated at S403/404 and S409/10 exclusively labeled pathological inclusions. This is in agreement with previous reports that TDP-43 is phosphorylated in abnormal aggregates [2, 11, 12, 17, 23, 25].



**Table 3** Staining pattern with various TDP-43 antibodies

Antibody	Epitope	Nuclei	NCI	DN	NFT	TANC	SF
TDP-43 (Abnova)	Full-length recombinant protein	++	+++	++	+	++	0
TDP-43 (ProteinTech)	Recombinant protein	+++	+++	++	+++	++	0
TDP-43 pS403/04	pTDP-43 (398–408, pS403/404)	0	+++	+++	++	++	+
TDP-43 pS409/10	pTDP-43 (405–414, pS409/410)	0	+++	+++	+	++	+
TDP-43 pS409/10 (monoclonal)	pTDP-43 (405–414, pS409/410)	0	+++	++	++	++	+
Anti-TDP-43N (3–12)	TDP-43 (N-terminal)	++	++	+	–	+	0
Anti-TDP-43C (405–414)	TDP-43 (C-terminal)	+	+++	++	++	++	+

Number of stained objects: 0, none; +, rare; ++, intermediate; +++, numerous

NCI Neuronal cytoplasmic inclusions, DN dystrophic neurites, NFT neurofibrillary tangles, TANC tangle associated neuritic clusters, SF star fish-shaped inclusions

We found that the antibodies directed against TDP-43 C-terminal epitopes (including phosphorylation-dependent epitopes) label a higher number of pathological inclusions compared to the antibody against the N-terminus. Although variations in antibody affinity could be the cause, enrichment of C-terminal fragments in inclusions has been previously reported [16, 18, 23, 25].

It is interesting to note that the distribution of TDP-43 inclusions parallels that of tau, and not that of ABri amyloid. Despite having a heavy amyloid load, the cerebellum is free of TDP-43 (and tau) inclusions. This could point to differences in the propensity of the particular neuron types to accumulate and develop inclusions, be it tau, TDP-43 or alpha-synuclein.

Co-deposition of TDP-43 with tau, alpha-synuclein or huntingtin does not necessarily imply a direct interaction between these molecules. Instead it may suggest that common pathological mechanisms act which lead to the aggregation of various abnormal proteins in susceptible neurons.

**Acknowledgments** We greatly appreciate the expert support with confocal imaging of Dr. Henry G. S. Martin (Vancouver, Canada). This research was supported by the Pacific Alzheimer Research Foundation.

**Conflict of interest statement** The authors declare that they have no conflict of interest.

## References

- Amador-Ortiz C, Lin WL, Ahmed Z et al (2007) TDP-43 immunoreactivity in hippocampal sclerosis and Alzheimer's disease. *Ann Neurol* 61:435–445
- Arai T, Hasegawa M, Akiyama H et al (2006) TDP-43 is a component of ubiquitin-positive tau-negative inclusions in frontotemporal lobar degeneration and amyotrophic lateral sclerosis. *Biochem Biophys Res Commun* 351:602–611
- Arai T, Mackenzie IR, Hasegawa M et al (2009) Phosphorylated TDP-43 in Alzheimer's disease and dementia with Lewy bodies. *Acta Neuropathol* 117:125–136
- Buratti E, Baralle FE (2001) Characterization and functional implications of the RNA binding properties of nuclear factor TDP-43, a novel splicing regulator of CFTR exon 9. *J Biol Chem* 276:36337–36343
- Buratti E, Baralle FE (2008) Multiple roles of TDP-43 in gene expression, splicing regulation, and human disease. *Front Biosci* 13:867–878
- Forman MS, Trojanowski JQ, Lee VM (2007) TDP-43: a novel neurodegenerative proteinopathy. *Curr Opin Neurobiol* 17:548–555
- Freeman SH, Spires-Jones T, Hyman BT, Growdon JH, Frosch MP (2008) TAR-DNA binding protein 43 in Pick disease. *J Neuropathol Exp Neurol* 67:62–67
- Fujishiro H, Uchikado H, Arai T et al (2009) Accumulation of phosphorylated TDP-43 in brains of patients with argyrophilic grain disease. *Acta Neuropathol* 117:151–158
- Geser F, Winton MJ, Kwong LK et al (2008) Pathological TDP-43 in parkinsonism-dementia complex and amyotrophic lateral sclerosis of Guam. *Acta Neuropathol* 115:133–145
- Griffiths RA, Mortimer TF, Oppenheimer DR, Spalding JM (1982) Congophilic angiopathy of the brain: a clinical and pathological report on two siblings. *J Neurol Neurosurg Psychiatry* 45:396–408
- Hasegawa M, Arai T, Akiyama H et al (2007) TDP-43 is deposited in the Guam parkinsonism-dementia complex brains. *Brain* 130:1386–1394
- Hasegawa M, Arai T, Nonaka T et al (2008) Phosphorylated TDP-43 in frontotemporal lobar degeneration and amyotrophic lateral sclerosis. *Ann Neurol* 64:60–70
- Higashi S, Iseki E, Yamamoto R et al (2007) Concurrence of TDP-43, tau and alpha-synuclein pathology in brains of Alzheimer's disease and dementia with Lewy bodies. *Brain Res* 1184:284–294
- Holton JL, Ghiso J, Lashley T et al (2001) Regional distribution of amyloid-Bri deposition and its association with neurofibrillary degeneration in familial British dementia. *Am J Pathol* 158:515–526
- Hu WT, Josephs KA, Knopman DS et al (2008) Temporal lobar predominance of TDP-43 neuronal cytoplasmic inclusions in Alzheimer disease. *Acta Neuropathol* 116:215–220
- Igaz LM, Kwong LK, Xu Y et al (2008) Enrichment of C-terminal fragments in TAR DNA-binding protein-43 cytoplasmic inclusions in brain but not in spinal cord of frontotemporal lobar degeneration and amyotrophic lateral sclerosis. *Am J Pathol* 173:182–194
- Inukai Y, Nonaka T, Arai T et al (2008) Abnormal phosphorylation of Ser409/410 of TDP-43 in FTL-DU and ALS. *FEBS Lett* 582:2899–2904
- Kwong LK, Neumann M, Sampathu DM, Lee VM, Trojanowski JQ (2007) TDP-43 proteinopathy: the neuropathology underlying major forms of sporadic and familial frontotemporal lobar degeneration and motor neuron disease. *Acta Neuropathol* 114:63–70
- Mackenzie IR, Baborie A, Pickering-Brown S et al (2006) Heterogeneity of ubiquitin pathology in frontotemporal lobar

- degeneration: classification and relation to clinical phenotype. *Acta Neuropathol* 112:539–549
20. Mackenzie IR, Neumann M, Bigio EH et al (2009) Nomenclature for neuropathologic subtypes of frontotemporal lobar degeneration: consensus recommendations. *Acta Neuropathol* 117:15–18
  21. Miklossy J, Steele JC, Yu S et al (2008) Enduring involvement of tau, beta-amyloid, alpha-synuclein, ubiquitin and TDP-43 pathology in the amyotrophic lateral sclerosis/parkinsonism-dementia complex of Guam (ALS/PDC). *Acta Neuropathol* 116:625–637
  22. Nakashima-Yasuda H, Uryu K, Robinson J et al (2007) Co-morbidity of TDP-43 proteinopathy in Lewy body related diseases. *Acta Neuropathol* 114:221–229
  23. Neumann M, Kwong LK, Lee EB et al (2009) Phosphorylation of S409/410 of TDP-43 is a consistent feature in all sporadic and familial forms of TDP-43 proteinopathies. *Acta Neuropathol* 117:137–149
  24. Neumann M, Mackenzie IR, Cairns NJ et al (2007) TDP-43 in the ubiquitin pathology of frontotemporal dementia with VCP gene mutations. *J Neuropathol Exp Neurol* 66:152–157
  25. Neumann M, Sampathu DM, Kwong LK et al (2006) Ubiquitinated TDP-43 in frontotemporal lobar degeneration and amyotrophic lateral sclerosis. *Science* 314:130–133
  26. Ou SH, Wu F, Harrich D, Garcia-Martinez LF, Gaynor RB (1995) Cloning and characterization of a novel cellular protein, TDP-43, that binds to human immunodeficiency virus type 1 TAR DNA sequence motifs. *J Virol* 69:3584–3596
  27. Oyanagi K, Makifuchi T, Ohtoh T, Chen KM, Gajdusek DC, Chase TN (1997) Distinct pathological features of the gallyas- and tau-positive glia in the Parkinsonism-dementia complex and amyotrophic lateral sclerosis of Guam. *J Neuropathol Exp Neurol* 56:308–316
  28. Plant GT, Revesz T, Barnard RO, Harding AE, Gautier-Smith PC (1990) Familial cerebral amyloid angiopathy with nonneuritic amyloid plaque formation. *Brain* 113:721–747
  29. Schnell SA, Staines WA, Wessendorf MW (1999) Reduction of lipofuscin-like autofluorescence in fluorescently labeled tissue. *J Histochem Cytochem* 47:719–730
  30. Schwab C, Arai T, Hasegawa M, Yu S, McGeer PL (2008) Colocalization of transactivation-responsive DNA-binding protein 43 and huntingtin in inclusions of Huntington disease. *J Neuropathol Exp Neurol* 67:1159–1165
  31. Schwab C, Hosokawa M, Akiyama H, McGeer PL (2003) Familial British dementia: colocalization of furin and ABri amyloid. *Acta Neuropathologica* 106:278–284
  32. Strong MJ, Volkening K, Hammond R et al (2007) TDP43 is a human low molecular weight neurofilament (hNFL) mRNA-binding protein. *Mol Cell Neurosci* 35:320–327
  33. Uryu K, Nakashima-Yasuda H, Forman MS et al (2008) Concomitant TAR-DNA-binding protein 43 pathology is present in Alzheimer disease and corticobasal degeneration but not in other tauopathies. *J Neuropathol Exp Neurol* 67:555–564
  34. Vidal R, Frangione B, Rostagno A et al (1999) A stop-codon mutation in the BRI gene associated with familial British dementia. *Nature* 399:776–781
  35. Worster-Drought C, Hill TR, McEnemey WH (1933) Familial presenile dementia with spastic paralysis. *J Neurol Psychopathol* 14:27–34

## TDP-43 in ubiquitinated inclusions in the inferior olives in frontotemporal lobar degeneration and in other neurodegenerative diseases: a degenerative process distinct from normal ageing

Yvonne Davidson · Hanan Amin · Thomas Kelley · Jing Shi · Jinzhou Tian · Ravindran Kumaran · Tammarny Lashley · Andrew J. Lees · Daniel DuPlessis · David Neary · Julie Snowden · Haruhiko Akiyama · Tetsuaki Arai · Masato Hasegawa · Rina Bandopadhyay · Steve Sikkink · Stuart Pickering-Brown · David M. A. Mann

Received: 20 August 2008 / Revised: 18 March 2009 / Accepted: 22 March 2009  
© Springer-Verlag 2009

**Abstract** Ubiquitin immunoreactive (UBQ-ir) inclusions were present to variable extents in the inferior olivary nucleus (ION) in 37/48 (77%) patients with frontotemporal lobar degeneration (FTLD), in 10/11 (91%) patients with motor neurone disease (MND), in 5/5 (100%) patients with Alzheimer's disease (AD), 5/7 (71%) patients with dementia with Lewy bodies, 13/19 (68%) patients with Parkinson's disease, 11/11 (100%) patients with Progressive

Supranuclear Palsy, 2/6 (33%) patients with Multisystem Atrophy, 1/3 (33%) patients with Huntington's disease and in 14/14 (100%) normal elderly control subjects. In FTLD, UBQ-ir inclusions were present in 26/32 (81%) patients with FTLD-U, in 10/15 (67%) patients with tauopathy, and in the single patient with Dementia Lacking Distinctive Histology. In 13 FTLD-U patients, and in a single AD and in 2 MND patients, the UBQ-ir inclusions had a rounded, spicular or skein-type appearance, and these were also TDP-43 immunoreactive (TDP-43-ir). In all other affected patients in all diagnostic groups, and in control subjects, the UBQ-ir neuronal cytoplasmic inclusions (NCI) were of a conglomerated type, resembling a cluster of large granules or globules, but were never TDP-43-ir. In 3 of the 13 FTLD-U patients with spicular NCI, conglomerated NCI were also present but in separate cells. Double-labelling immunohistochemistry, and confocal microscopy, for UBQ and TDP-43 confirmed that only the spicular UBQ-ir inclusions in patients with FTLD-U, AD and MND contained TDP-43, though in these patients there were occasional TDP-43 immunoreactive inclusions that were not UBQ-ir. Nuclear TDP-43 immunoreactivity was absent in ION in FTLD-U, AD or MND when TDP-43 cytoplasmic inclusions were present, but remained in neurones with UBQ-ir, TDP-43 negative inclusions. The target protein within the UBQ-ir, TDP-43-negative inclusions remains unknown, but present studies indicate that this is not tau, neurofilament or internexin proteins. These TDP-43 negative, UBQ-ir inclusions appear to be more related to ageing than neurodegeneration, and are without apparent diagnostic significance. The pathophysiological mechanism leading to their formation, and any consequences their presence may have on nerve cell function, remain unknown.

Y. Davidson · H. Amin · T. Kelley · J. Shi · J. Tian · D. DuPlessis · D. Neary · J. Snowden · D. M. A. Mann (✉)  
Clinical Neuroscience Research Group, Faculty of Medical and Human Sciences, Greater Manchester Neurosciences Centre, School of Translational Medicine, Hope Hospital, University of Manchester, Salford M6 8HD, UK  
e-mail: david.mann@manchester.ac.uk

S. Sikkink · S. Pickering-Brown  
Clinical Neuroscience Research Group, Faculty of Medical and Human Sciences, School of Translational Medicine, University of Manchester, Stopford Building, Oxford Rd, Manchester M13 9PT, UK

J. Shi · J. Tian  
The Neurology Centre, Dongzhimen Hospital, Beijing University of Chinese Medicine, 5 Hyuncang St, 100700 Beijing, People's Republic of China

R. Kumaran · T. Lashley · A. J. Lees · R. Bandopadhyay  
Reta Lila Weston Institute for Neurological Studies, Institute of Neurology, 1 Wakefield St, London WC1 1PJ, UK

H. Akiyama · T. Arai  
Department of Psychogeriatrics, Tokyo Institute of Psychiatry, 2-1-8 Kamikitazawa, Setagaya-ku, Tokyo 156-8585, Japan

M. Hasegawa  
Department of Molecular Neuropathology, Tokyo Institute of Psychiatry, 2-1-8 Kamikitazawa, Setagaya-ku, Tokyo 156-8585, Japan

## Introduction

Frontotemporal Lobar Degeneration (FTLD) is a descriptive term that is widely used to refer to a heterogeneous group of non-Alzheimer forms of dementia with onset of illness usually before 65 years of age arising from the degeneration of the frontal and temporal lobes. Although many cases of FTLD show insoluble tau proteins in their brains in the form of intraneuronal neurofibrillary tangles or Pick bodies (known as FTLD-tau [29], a tau-negative histology, in the form of (UBQ)-immunoreactive (UBQ-ir) neuronal cytoplasmic inclusions (NCI) and/or neuritic changes in the outer laminae of the frontal and temporal cortex, and in the dentate gyrus of the hippocampus—a pathology referred to as FTLD-U or FTLD-MND when clinical motor neurone disease (MND) is also present—more commonly underlies FTLD [8, 13, 15, 16, 18, 21, 26, 28, 29, 37, 43, 45]. In some FTLD-U cases, neuronal intranuclear inclusions (NII) of a “cat’s eye” or “lentiform” appearance have been described [24, 25, 47], especially in those cases with autosomal dominant inheritance associated with mutations in progranulin gene (*PGRN*) [3, 5, 9, 27, 38, 41, 44]. The presence of UBQ-ir NCI within anterior horn cells of the spinal cord, and motor neurones of certain cranial nerve nuclei, has long been recognised as a principal pathological change in patients with classic MND [20, 23, 25], and similar UBQ-ir NCI can be seen in these neurones in patients with FTLD-MND and FTLD-U [43]. UBQ-ir inclusions have also been observed in neurones of superior and inferior olivary nuclei (ION) in some patients with FTLD-U, FTLD-MND and MND alone [10, 11, 25].

Biochemical and immunohistochemical analyses have shown the TAR DNA-binding protein, TDP-43, to be a major constituent of the UBQ-ir lesions of the cerebral cortex and hippocampus in most cases of FTLD-U and FTLD-MND [2, 10, 40], and such cases are now classed as FTLD-TDP [29]. Importantly, this same protein is present in NCI in anterior horn cells and cranial nerve motor neurones in patients with MND alone [2, 10, 40]. It has been noted that at least some inclusions within ION also appear to contain TDP-43 protein [10]. However, the specificity of NCI in ION in relationship to FTLD clinical and histological phenotype, and their relevance to disease symptomatology, remains to be clarified.

In this present study, we have investigated the frequency and composition of UBQ-ir NCI within the ION in patients with FTLD-TDP compared to patients with FTLD-tau (i.e., patients with familial FTDP-17 associated with *MAPT* mutation, or sporadic FTLD with Pick bodies), and to patients with a range of other neurodegenerative diseases, such as classic MND, Alzheimer’s disease (AD), Dementia with Lewy bodies (DLB), Parkinson’s disease (PD),

Progressive Supranuclear Palsy (PSP), Multi System Atrophy (MSA) and Huntington’s disease (HD), and in mentally and neurologically normal elderly persons. In this way, we have determined whether the presence of UBQ-ir NCI within the ION is specific to patients with (particular forms of) FTLD, is a feature widely observed in neurodegenerative disease, or is present ‘simply’ as an aspect of growing older irrespective of the presence of neurological illness.

## Materials and methods

Blocks of medulla oblongata (at the level of the hypoglossus nerve nucleus) were cut from the brains of 124 patients, 74 drawn from the Manchester Brain Bank and 50 from the UK Parkinson’s Disease Society Tissue Bank. All brains had been collected with Local Research Ethical Committee approval, and had been fixed in 10% buffered formaldehyde for at least 3–4 weeks before cutting. The study group was comprised of 48 patients with sporadic and familial FTLD [7, 8, 39] (28 males, 20 females, age 31–78 years, mean  $65.3 \pm 8.3$  years), 11 with sporadic MND [6] (8 males, 3 females, age 45–72 years, mean  $65.4 \pm 10.4$  years), 5 with AD [34] (3 males, 2 females, age 59–86 years, mean  $68.6 \pm 10.6$  years), 7 with DLB [33] (4 males, 3 females, age 62–81 years, mean  $73.6 \pm 7.4$  years), 19 with PD [33] (12 males, 7 females, age 59–89 years, mean  $78.6 \pm 7.2$  years), 11 with PSP [22] (10 males, 1 female, age 66–90 years, mean  $79.0 \pm 8.4$  years), 6 with MSA [46] (4 males, 2 females, age 42–86 years, mean  $67.8 \pm 14.8$  years), 3 with (genetically verified) HD (2 males, 1 female, age 50–70 years, mean  $58.3 \pm 10.4$  years) and 14 neurologically normal control subjects (7 males, 7 females, age 58–93 years, mean  $78.9 \pm 8.8$  years); all diagnoses were made according to standard consensus clinical and pathological criteria.

Thirty-two patients (21 males, 11 females, age 45–77 years, mean  $66.0 \pm 8.8$  years) had tau-negative, FTLD-TDP histology (4 also had clinical MND, i.e., FTLD-MND). Nine of 32 FTLD-TDP patients had FTLD-U type 1 histology, 10 had FTLD-U type 2 histology and 13 had type 3 FTLD-U histology (see [8, 29] for details of classification system). Of 15 patients with FTLD-tau (7 males, 8 females, age 53–77 years, mean  $63.6 \pm 7.3$  years), 8 had Pick-type histology and 7 had neuronal and glial cell tangles (FTDP-17T) associated with exon 10 mutations in *MAPT*. One patient had DLDH. Clinically, 30 of the FTLD patients had FTD, 4 had FTD + MND, 8 had semantic dementia (SD) and 6 had progressive non-fluent aphasia (PNFA). Of the 30 patients with FTD, pathologically, 15 had tauopathy (8 with Pick body histology and 7 with FTDP-17T (6 patients had

*MAPT* exon 10 +16 mutation and 1 had *MAPT* exon 10 +13 mutation), 14 had FTL-D-TDP and 1 had DLDH. All 4 patients with FTD + MND, all 8 patients with SD and all 6 patients with PNFA had FTL-D-TDP.

Five patients with FTL-D-TDP (3 with FTD and 2 with PNFA) had *PGRN* mutations. Two FTD patients had exon 10 V452WfsX38 mutation, and 1 had exon 11 R493X mutation. The PNFA patients had exon 1C31LfsX34 mutation, and exon 4 Q130SfsX124 mutation.

The clinical, demographic, histopathological and genetic characteristics of these FTL-D patients have recently been described by us [3, 10, 26, 28, 43, 45].

Tissue blocks were processed routinely into paraffin wax and sections cut at a thickness of 5  $\mu$ m. Sections were immunostained for UBQ using a polyclonal anti-UBQ antibody (Dako, Glostrup, Denmark, 1:500) (see [28] for details). Other sections from these same patients were immunostained for TDP-43 using a commercially available phospho-independent TDP-43 polyclonal antibody (10782-1-AP, Proteintech Inc, Chicago, IL) at a dilution of 1:1000 (see [10] for details). Selected sections from cases with high density of UBQ-ir/TDP-ir inclusions in ION were also immunostained [10] for phosphorylated TDP-43 using the phospho-dependent TDP-43 antibody pS409/410-2 (Cosmobio Co Ltd, Tokyo) at a dilution of 1:1,000. Other, similarly selected sections were immunostained for p62 protein using a commercially available polyclonal antibody [p62 lck ligand (610832), BD Biosciences Europe, Oxford] at a dilution of 1:100. To enhance p62 immunoreaction, sections were again microwaved in 0.1 M citrate buffer, pH 6.0 prior to incubation in primary antibody (see [10] for details). Other sections from these selected cases were immunostained for phosphorylated tau (AT8, Innogenetics, Antwerp 1:500), neurofilament protein (SMI31, Sternberger Meyer Immunochemicals 1:200),  $\alpha$ -synuclein (Novocastra, UK 1:500),  $\alpha$ -internexin (Zymed Laboratories Inc, San Francisco, USA 1:200) as described elsewhere [43]. In all instances, subsequent steps in the immunoreaction were performed using Vector Elite secondary antibody kit with DAB as revealing agent. Sections were then lightly counterstained with haematoxylin.

For selected cases, double immunolabelling was performed. TDP-43 immunoreaction was first performed, as above, with DAB as revealing agent. This was followed by UBQ immunoreaction employing mouse monoclonal UBQ antibody (NCL-UBIQm, Vision Biosciences, Newcastle, UK, 1:50), with Vector Elite secondary antibody kit with very intense purple (VIP) as revealing agent. Sections were again lightly counterstained with haematoxylin.

Immunofluorescence confocal microscopy was performed on selected (representative) cases with UBQ-ir, TDP-43 positive or TDP-43 negative inclusions. Double immunofluorescence was carried out using TDP-43 and

UBQ antibodies sequentially. TDP-43 signal was visualised using tetramethyl rhodamine labelled secondary antibody and UBQ with the fluorescein signal amplification kit (Perkin Elmer, UK). Sections were washed thoroughly in phosphate buffered saline and mounted in aquamount (Merck, UK). Control sections incubated without primary antibody exhibited no significant background staining. Fluorescent signals from sections were scanned using a Leica SP2 laser confocal microscope with Leica LCS software.

The severity of UBQ and TDP-43 pathology within the ION was rated semiquantitatively:

0 = absent, no inclusions present on either side of ION  
0.5 = rare, just one or two inclusions present in either or both sides of ION.

1 = mild, 2–5 inclusions present in ION on either side.  
2 = moderate, 5–10 inclusions present in ION on either side;

3 = severe, 10–15 inclusions present in ION on either side.

4 = very severe, more than 15 inclusions present.

All statistical tests were performed using SSPS 13.0.

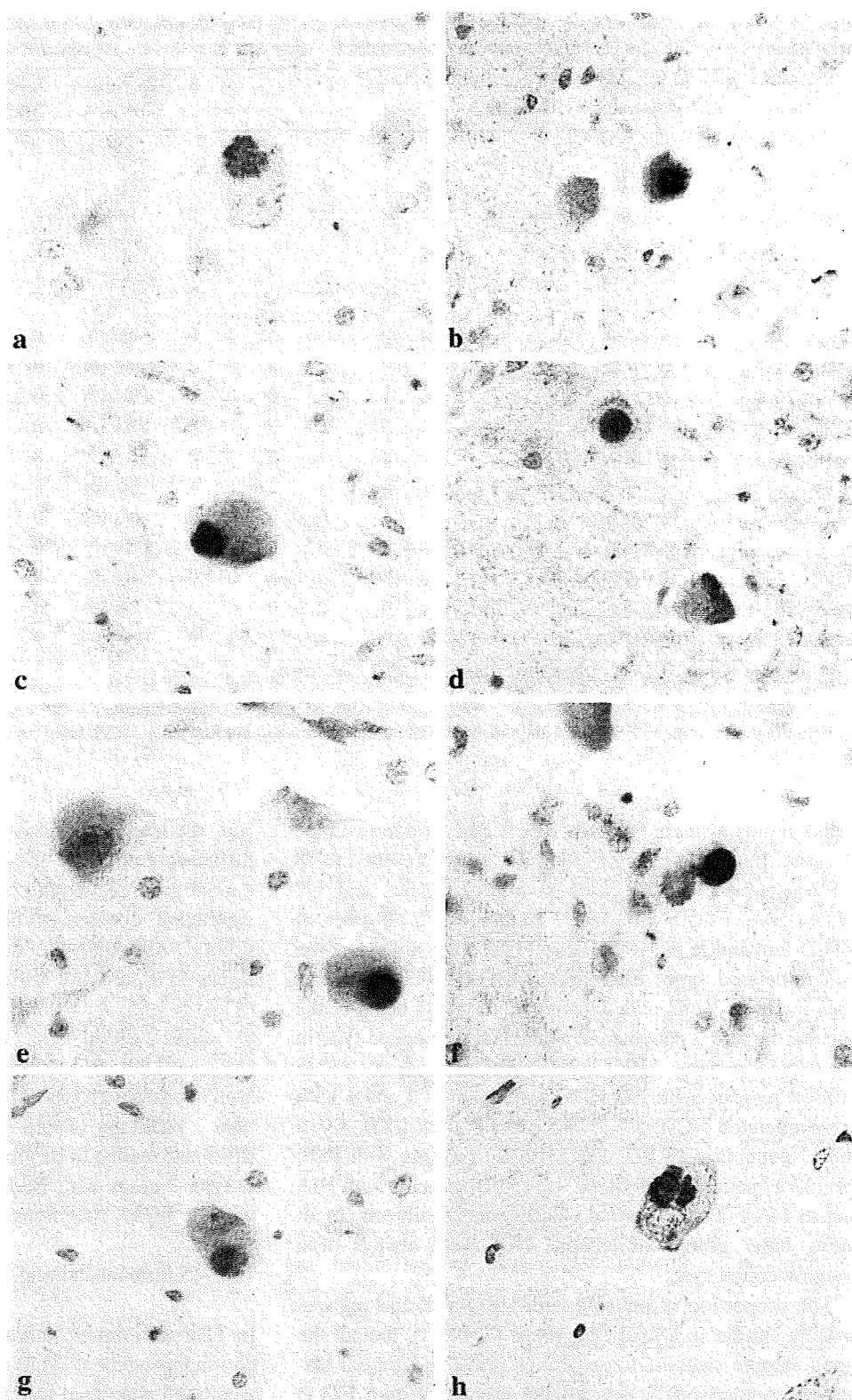
## Results

### UBQ immunostaining

Within ION, NCI adopted two morphologies on UBQ immunostaining (UBQ-ir). Most often, they appeared as a single clump, or a cluster, of small granules or larger globules (known henceforth as 'conglomerated NCI') (Fig. 1a). However, on other occasions, UBQ-ir NCI were of a more solid, rounded appearance (Fig. 1c) often spicular (Fig. 1b), sometimes more skein-like (Fig. 1d) (known henceforth as 'spicular NCI'). 'Ghost' cells containing spicular UBQ-ir NCI, but without apparent organelles, were occasionally present (Fig. 1c) and spicular UBQ-ir extracellular NCI were sometimes seen (Fig. 1d). The conglomerated type of NCI were sometimes visible on haematoxylin–eosin staining, but not consistently so across all cases.

UBQ-ir inclusions (conglomerated or spicular, or both) were seen in 37/48 (77%) FTL-D cases, these being present in 26/32 (81%) FTL-D-TDP cases (including 1/4 FTL-D-MND cases), in 10/15 (67%) FTL-D-tau cases, and in the single DLDH case. With respect to FTL-D-TDP cases, spicular NCI were (often widely) present in 12/13 patients with FTL-D-U type 3 histology (i.e., those cases with a moderate number, or numerous, UBQ-ir NCI and neurites within the cerebral cortex—see [8, 29]), including all 5 with *PGRN* mutations. The conglomerated type of NCI was also seen in 2 of these 12 patients, but always in separate

**Fig. 1** Neuronal cytoplasmic inclusions (NCI) in neurones of the inferior olivary nucleus. On UBQ immunostaining two distinct types of NCI are present; one type (a) appears as a cluster or conglomerate of small granules or globules, while the other type (b–d) has a more solid, rounded, sometimes spicular or skein-like, appearance. 'Ghost' cells containing spicular NCI (c) and extracellular NCI (d) are sometimes seen. The rounded, spicular NCI are TDP-43 immunoreactive (e, f) and occasional neurones undergoing neuronophagia with liberation of NCI into extracellular space are seen (f). Both the rounded, spicular (g) and conglomerated (h) NCI are p62 immunoreactive. Microscope objective magnification  $\times 40$



cells from those with spicular NCI. Conglomerated UBQ-ir NCI were also seen in 8/9 patients with FTLD-U type 1 histology (i.e., those with numerous, UBQ-ir neurites but few NCI within the cerebral cortex [8]) and in 6/10 patients

with FTLD-U type 2 histology (i.e., those with numerous, UBQ-ir NCI but few or no neurites within the cerebral cortex [8, 29]). These were usually of the conglomerated type, and spicular NCI were present (again in separate